Published in final edited form as:
*J Med Chem*. 2012 July 12; 55(13): 6149–6161. doi:10.1021/jm300608w.

# Structure-based Design of Potent Bcl-2/Bcl-xL Inhibitors with Strong *in vivo* Antitumor Activity

**Haibin Zhou**[+,∞], **Angelo Aguilar**[+,∞], **Jianfang Chen**[+,∞], **Longchuan Bai**[+,∞], **Liu Liu**[+,∞], **Jennifer L. Meagher**[#,∞], **Chao-Yie Yang**[+,∞], **Donna McEachern**[+], **Xin Cong**[+], **Jeanne A. Stuckey**[#,€], and **Shaomeng Wang**[+,*]

[+]Comprehensive Cancer Center and Departments of Internal Medicine, Pharmacology and Medicinal Chemistry, University of Michigan, 1500 E. Medical Center Drive, Ann Arbor, MI 48109-0934, USA

[#]Life Sciences Institute, University of Michigan, 1500 E. Medical Center Drive, Ann Arbor, MI 48109-0934, USA

## Abstract

Bcl-2 and Bcl-xL are key apoptosis regulators and attractive cancer therapeutic targets. We have designed and optimized a class of small-molecule inhibitors of Bcl-2 and Bcl-xL containing a 4,5-diphenyl-1*H*-pyrrole-3-carboxylic acid core structure. A 1.4 Å resolution crystal structure of a lead compound, **12**, complexed with Bcl-xL has provided a basis for our optimization. The most potent compounds, **14** and **15**, bind to Bcl-2 and Bcl-xL with subnanomolar $K_i$ values and are potent antagonists of Bcl-2 and Bcl-xL in functional assays. Compounds **14** and **15** inhibit cell growth with low nanomolar $IC_{50}$ values in multiple small-cell lung cancer cell lines and induce robust apoptosis in cancer cells at concentrations as low as 10 nM. Compound **14** also achieves strong antitumor activity in an animal model of human cancer.

## Introduction

Apoptosis resistance is a hallmark of human cancer,[1–4] and targeting key anti-apoptosis regulators with the goal of restoring apoptosis in cancer cells is a promising new therapeutic approach to cancer.[5, 6]

The Bcl-2 proteins are key regulators of apoptosis and consist of both anti- and pro-apoptotic members.[2, 7] The anti-apoptotic proteins include Bcl-2, Bcl-xL, Bcl-w, Mcl-1 and A1, while the pro-apoptotic members consist of BID, BIM, BAD, BAK, BAX and NOXA, among others.[7] The balance and their interaction between the pro-apoptotic members and the anti-apoptotic members within the Bcl-2 family of proteins control cell fate. [2, 7] Upon receipt of apoptotic stimuli, the pro-apoptotic proteins BAX and/or BAK disrupt the integrity of the outer mitochondrial membrane by forming oligomers in this membrane, and this leads to the release of the pro-apoptotic signaling proteins cytochrome c and Smac, and activation of downstream caspases. Overexpression of the anti-apoptotic Bcl-2 and Bcl-xL proteins in cancer cells inhibits apoptosis by blocking activation of BAX and/or BAK and confers cancer cells resistance to a variety of chemotherapeutic agents.[8, 9] It has been proposed that small molecules that block the interaction of Bcl-2/Bcl-xL proteins with pro-

[*]To whom correspondence should be addressed: Tel: 734-615-0362, Fax: 734-647-9647, shaomeng@umich.edu. [€]To whom correspondence should be addressed for x-ray crystallography study.
[∞]Equal contribution

Supporting Information (SI) Available: Experimental procedures and spectral data. This material is available free of charge via the Internet at http://pubs.acs.org.

apoptotic Bcl-2 proteins can antagonize the anti-apoptotic function of Bcl-2/Bcl-xL proteins and overcome apoptosis resistance mediated by overexpression of Bcl-2/Bcl-xL in tumor cells.[8, 9] Design of potent, cell-permeable small-molecule Bcl-2/Bcl-xL inhibitors has been the subject of intense efforts in the last decade.[10] Compound **1** (ABT-737, Figure 1) and its analogue **2** (ABT-263, Figure 1) are probably the two most potent Bcl-2/Bcl-xL inhibitors reported to date.[11–13] Both compounds bind to Bcl-2 and Bcl-xL with high affinities and have a weak affinity for Mcl-1. Compound **2** has been advanced into Phase I/II clinical trials for the treatment of human cancer.[14, 15] The recently synthesized quinazoline sulfonamide **3** (Figure 1) also shows high binding affinities to Bcl-2 and Bcl-xL and a weak affinity to Mcl-1.[16]

We recently reported the design of a new class of Bcl-2/Bcl-xL inhibitors, exemplified by compounds **4**, **5** and **6** (Figure 1), with **6** being the most potent one among them.[17] Although compound **6** binds to Bcl-2 and Bcl-xL with subnanomolar affinities ($K$i < 1 nM) and potently inhibits cell growth in the H146 small-cell lung cancer cell line with an $IC_{50}$ value of 60 nM,[17] it fails to induce robust apoptosis in the H146 xenograft tumor tissues at its maximum tolerated dose (data not shown). In this paper, we report further structure-based design, synthesis and evaluation of a set of new Bcl-2/Bcl-xL inhibitors. The best new compound not only binds to Bcl-2/Bcl-xL with subnanomolar affinities and effectively induces apoptosis in tumor cells, but also achieves strong antitumor activity in an animal model of human cancer.

## Results and Discussion

We have previously determined the crystal structure of compound **7** complexed with Bcl-xL (Figure 2A) and used the crystal structure for the design of compounds **4**, **5** and **6**. Analysis of this crystal structure (Figure 2A) suggested that the 3,4-diphenyl-1*H*-pyrrole in **7** can be changed to 4,5-diphenyl-1*H*-pyrrole for effective interaction with Bcl-xL. Because the dihydroxybutyl side chain in **7** lacks any specific interaction with the Bcl-xL protein in the crystal structure, it was truncated to a methyl group. The piperazine group was retained because it enhances the aqueous solubility of compounds containing it. These changes led to compound **8** (Figure 3). Compound **8** binds to Bcl-2 and Bcl-xL with $K_i$ values of 38 μM and 88 μM, respectively, 2 times more potent than **7** and was used as the lead structure in subsequent design. Using the crystal structure of **7** complexed with Bcl-xL as a starting point, we developed a model of compound **8** complexed with Bcl-xL (Figure 2B).

In our previous study, we designed compound **4** by tethering **7** with a portion of **1**, which occupies two different binding pockets in Bcl-xL.[17] Using a similar strategy, we have designed **9** by tethering **8** with the same portion of **1** used for the design of **4**. Compound **9** binds to Bcl-2 and Bcl-xL proteins, with $K_i$ values of 7 nM and 1.3 nM, respectively (Table 1). Our previous study further showed that removal of the carbonyl group in the linker region in **4**, which yielded **5**, improves both binding affinities to Bcl-2 and Bcl-xL, and cellular activity. Thus, we synthesized **10** by removal of the corresponding carbonyl group in compound **9**. Compound **10** binds to Bcl-2 ($K_i$ <1 nM) and Bcl-xL ($K_i$ = 2.4 nM) and is more potent than compound **9** in binding to Bcl-2. Both compounds **9** and **10** also show a high specificity over Mcl-1, with $IC_{50}$ values >10 μM (Table 1).

We evaluated compounds **8**, **9** and **10** for their activity in cell growth inhibition in three small-cell lung cancer cell lines (H146, H1417 and H1963), which have been shown to be sensitive to potent and specific Bcl-2/Bcl-xL inhibitors such as compounds **1** and **2**. Compound **10** inhibits cell growth in these three small-cell lung cancer lines with $IC_{50}$ values of 110, 258 and 72 nM, respectively (Table 1). In comparison to **10**, compound **9** is much less effective against these three cell lines ($IC_{50}$ > 10 μM). Consistent with its weak

binding affinities to Bcl-2 and Bcl-xL, compound **8** has minimal cellular activity (Table 1). Compound **1** has $IC_{50}$ values of 37, 412 and 59 nM, respectively, in these three cancer cell lines (Table 1).

To provide direct evidence that compound **10** antagonizes Bcl-2 and Bcl-xL but not Mcl-1, we have established cell-free functional assays using purified mitochondria, recombinant Bcl-2/Bcl-xL/Mcl-1 proteins and the BIM BH3 peptide, which binds to Bcl-2, Bcl-xL and Mcl-1 with very high affinities (Table 1). We employed these cell-free functional assays to determine the functional antagonism of compounds **1** and **10**, and also of the BAD and the NOXA BH3 peptides.

At a concentration of 20 nM, the BIM BH3 peptide induces substantial release of cytochrome c and Smac proteins from mitochondria, and Bcl-2, Bcl-xL or Mcl-1, each at 60 nM, efficiently inhibits this release (Figure 4). In the Bcl-2 functional assay (Figure 4A), compounds **1** and **10** dose-dependently antagonize Bcl-2 and restore BIM-induced release of cytochrome c and Smac proteins from mitochondria, and **10** is 3-times less potent than **1**. The BAD BH3 peptide is capable of doing so in a dose-dependent manner, but the NOXA BH3 peptide fails to restore the release of cytochrome c and Smac. In the Bcl-xL functional assay (Figure 4B), compounds **1** and **10** antagonize Bcl-xL and restore the release of cytochrome c and Smac, but the NOXA BH3 peptide is unable to do so. Compounds **1** and **10** are equally effective in antagonizing Bcl-xL, but both compounds are less potent than the BAD BH3 peptide. In the Mcl-1 functional assay (Figure 4C), while the NOXA peptide antagonizes Mcl-1 and restores the release of cytochrome c and Smac induced by the BIM peptide in a dose-dependent manner, the BAD peptide, **1** and **10** at concentrations as high as 10 μM fail to do so. These data show that **1**, **10**, and the BAD peptide all function as potent antagonists of Bcl-2 and Bcl-xL proteins, but all fail to antagonize Mcl-1. On the other hand, while the NOXA peptide efficiently antagonizes Mcl-1, it fails to do so with both Bcl-2 and Bcl-xL proteins. These functional data are consistent with their binding profiles to these Bcl-2 proteins (Table 1).

We next embarked on modifications of **10** in order to further improve its binding affinities to Bcl-2 and Bcl-xL and its cellular activity against cancer cells. The results are summarized in Figure 5 and Table 1.

The 1-methyl-4-propylpiperazinyl side chain on the pyrrole ring of **10** was intended to enhance the aqueous solubility of the compound. This side chain was modified to examine its influence on binding and cellular activity, which led to the amide analogue **11** and the carboxylic acid analogue **12**. These both bind to Bcl-2 and Bcl-xL with very high binding affinities (Table 1), exceeding the lower limits of the assays except that compound **11** binds to Bcl-2 with a $K_i$ value of 1.1 nM. Compound **13**, in which the carboxyl group has been removed from the pyrrole ring in **12**, binds to Bcl-2 100 times less potently than **12**, but it is only slightly less potent than **12** in binding to Bcl-xL. These data indicate that the carboxyl group plays a critical role with respect to the binding to Bcl-2, but makes only a modest contribution to Bcl-xL binding.

Compounds **11** and **12** have similar potencies in the cell growth inhibition assay against the H146, H1417 and H1963 cancer lines and are 2–4 times more potent than compound **10**. Consistent with its low binding affinity to Bcl-2, compound **13** shows very weak activities (> 5 μM) in these three cancer cell lines.

To provide a solid structural basis for subsequent modifications, we have attempted to determine the crystal structures for these Bcl-2/Bcl-xL inhibitors (**10, 11** and **12**) complexed with Bcl-2 and/or Bcl-xL. We determined a crystal structure of **12** complexed with Bcl-xL at

a resolution of 1.4 Å (Figure 6 and Table S1 in SI). This crystal structure shows that the diphenylpyrrole core structure of **12** binds in the same pocket and with the same orientation as that of **7**. Adjacent to the *N*-methyl group on the pyrrole ring, there is an unoccupied hydrophobic pocket lined by L108, V126, F146, L112 and L150 which can be exploited for further optimization. In addition to the diphenylpyrrole core structure, the thiophenyl ring of **12** has extensive hydrophobic interactions with the protein. This thiophenyl ring is also involved in π-stacking with the nitrophenyl group in **12**, which presumably stabilizes the bound conformation of **12**. The dimethylamino group forms two hydrogen bonds with the carboxyl group of E96 but the nitro group on the phenyl ring fails to fill adequately the pocket in Bcl-xL lined by Y195, F191, W197, V141 and A141, suggesting the possibility of additional optimization at this site to further improve binding affinities and cellular activities. The carboxylic acid in **12** forms a direct hydrogen bond with R132 and an indirect hydrogen bond with R139 in Bcl-xL, mediated by a water molecule.

Based upon this crystal structure, the *N*-methyl group on the pyrrole ring binds in a hydrophobic pocket lined by L108, V126, F146, L112 and L150, but there is additional room available to accommodate a larger hydrophobic group. We therefore designed and synthesized three new analogues (compounds **14**, **15** and **16**) with an *N*-ethyl, *N*-isopropyl, or *N*-cyclopropyl group (Figure 5). Compounds **14** and **15** bind to both Bcl-2 and Bcl-xL with very high affinities ($K_i$ < 1nM), exceeding the lower limits of the assays. While compound **16** binds to Bcl-2 with 10-times lower affinity than **12**, they both have similar affinities to Bcl-xL.

Consistent with their high binding affinities to both Bcl-2 and Bcl-xL, both compounds **14** and **15** are very potent in cell growth inhibition in the H146, H1417 and H1963 cancer cell lines. While compound **14** has $IC_{50}$ values of 8.1, 17.7 and 4.5 nM, respectively, compound **15** achieves $IC_{50}$ values of 3.0, 3.4 and 1.9 nM (Table 1 and Figure 7A). Compound **16** has much weaker cell growth inhibitory activity than compounds **14** and **15** against these three cancer cell lines, which is consistent with its weaker binding affinity to Bcl-2 than **14** and **15**. In direct comparison, compound **15** is 10–100 times more potent than compound **1** against these three cancer cell lines in the cell growth inhibition assay, representing arguably the most potent Bcl-2/Bcl-xL inhibitor reported to date.

We next evaluated the ability of compounds **12**, **14**, **15** and **1** to induce cell death in the H146 cell line (Figure 7B). These four compounds all effectively induce cell death in H146 in a dose-dependent manner. While compounds **12** and **1** have similar potencies to each other, **14** and **15** are more potent than both **12** and **1** and, even at 10 nM, induce robust cell death in the H146 cell line. Western blotting analysis further showed that while all these four compounds induce cleavage of caspase-3 and poly (ADP- ribose) polymerase (PARP) in a dose-dependent manner (Figure 7C), compound **15** induces robust cleavage of caspase-3 and PARP at concentrations as low as 10 nM, and is more potent than compounds **12** and **1**.

To further probe their cellular mechanism of action, we analyzed release of cytochrome C from mitochondria, which is an early event in apoptosis induction. Treatment of H146 cells with compounds **14** and **15** for as short as 2 h induces a release of cytochrome C in a dose-dependent manner (Figure 8). This release of cytochrome C is accompanied by cleavage of PARP, also in a dose-dependent manner. Release of cytochrome C and cleavage of PARP are robust at concentrations of 30 nM for both **14** and **15**.

We evaluated the toxicity of compounds **14** and **15** in severe combined immune deficient (SCID) mice and found that **15** is more toxic than **14**. While compound **14** at 25 mg/kg, daily intravenous dosing and five days a week for 2 weeks is well tolerated in SCID mice,

**15** at the same dose and schedule is toxic to the animals which had severe weight loss. We therefore focused our subsequent *in vivo* evaluations on **14**.

We tested compound **14** for induction of apoptosis in the H146 xenograft tissues in SCID mice (Figure 9). A single intravenous dose of **14** at 25 mg/kg effectively induced cleavage of PARP and caspase-3 in the H146 tumor tissues as early as 3 h and lasted for at least 24 h.

Compound **14** was next evaluated for its antitumor activity in inhibition of tumor growth in the H146 xenograft model. It was administered at 25 mg/kg daily *i.v.* 5 days a week for 2 weeks. Compound **14** was very effective in inhibition of tumor growth (Figure 10), consistent with our *in vivo* pharmacodynamics data (Figure 9). In fact, compound **14** was capable of achieving tumor regression during the treatment phase. The strong antitumor activity of **14** is persistent. At day 92, 2 months after the treatment ended, the tumors treated with **14** had a mean volume of 200 $mm^3$, whereas the vehicle-treated tumors had grown to a mean volume of 800 $mm^3$. Mice treated with **14** had a maximum weight loss <10% during the treatment and animals quickly gained weight after the treatment (Figure S1 in SI). There were no other signs of toxicity observed with **14**. Hence, compound **14** has a strong antitumor activity at a well-tolerated dose-schedule.

## Synthesis

The synthesis of compound **8** is shown in Scheme 1. Condensation of ethyl acetoacetate with benzaldehyde afforded ethyl 2-benzylidene-3-oxobutanoate. A Stetter reaction of this compound with 4-chlorobenzaldehyde gave **17**, and the pyrrole **18** was obtained by Paal-Knorr cyclization of **17** with methylamine.[18] Compound **8** was prepared by hydrolysis of **18**, followed by coupling to 1-(3-aminopropyl)-4-methylpiperazine.

Scheme 2 shows the general method for the synthesis of compounds **12**, **14**, **15** and **16** with different substituents on the nitrogen of the pyrrole ring. Compound **19** was prepared in the same way as **17**. Paal-Knorr cyclization of **19** with different amines afforded the pyrroles **20a-d** which were hydrolyzed to yield the acids **21a-d**. An Ullmann-type C-N bond formation reaction[19] was employed to prepare intermediate **22a-d** from **21a-d**. Hydrogenation of the nitro group in **22a-d** gave the anilines, treatment of which with 4-fluoro-3-nitrobenzene-1-sulfonyl chloride in pyridine gave **23a-d**. Displacement of the fluoro group in **23a-d** with (*R*)-N′,N′-dimethyl-4-(phenylthio)butane-1,3-diamine produced compounds **12**, **14**, **15** and **16**.

Compound **9** was synthesized as shown in Scheme 3. Coupling **21a** to 1-(3-aminopropyl)-4-methylpiperazine afforded **24** and intermediate **25** was prepared as described.[20] In the presence of $Pd(dba)_2$ and tri-*tert*-butylphosphine, Buchwald–Hartwig reaction[21] between **24** and **25** produced compound **9**.

Syntheses of compounds **10**, **11** and **13** are outlined in Scheme 4. Compounds **10** and **11** were produced by coupling compound **12** to the corresponding amines using EDCI and HOBt. Treatment of compound **12** with TFA afforded the decarboxylated compound **13**.

## Summary

Using a structure-based design strategy, we have designed and synthesized new and potent Bcl-2/Bcl-xL inhibitors. The most potent compounds, **14** and **15**, bind to Bcl-2 and Bcl-xL with subnanomolar affinities and inhibit cell growth in three lung cancer cell lines with low nanomolar $IC_{50}$ values. Compounds **14** and **15** induce robust apoptosis in H146 cancer cells at concentrations as low as 10 nM. Furthermore, compound **14** induces robust apoptosis *in*

*vivo* in the H146 tumor tissues, and strongly inhibits tumor growth and achieves tumor regression during the treatment in the H146 xenograft model in mice at a well-tolerated dose-schedule. Determination of the 1.4 Å resolution crystal structure of a potent analogue, **12** complexed with Bcl-xL, provides a structural basis for its high-affinity binding to Bcl-xL and a solid foundation for our optimization effort. Further optimization of this class of compounds may yield highly potent Bcl-2/Bcl-xL inhibitors with optimized pharmacological properties for the treatment of human cancer.

## EXPERIMENTAL SECTION

### General Information

Unless otherwise stated, all reactions were performed under a nitrogen atmosphere in dry solvents under anhydrous conditions. Unless otherwise noted, reagents were used as supplied without further purification. NMR spectra were acquired at a proton frequency of 300 MHz and chemical shifts are reported in parts per million (ppm) relative to an internal standard. The final products were purified by a C18 reverse phase semi-preparative HPLC column with solvent A (0.1% of TFA in water) and solvent B (0.1% of TFA in $CH_3CN$) as eluents. The purity was determined by Waters ACQUITY UPLC and all the biologically evaluated compounds were > 95% pure (Table S2 and Figures S2–10).

**Ethyl 5-(4-chlorophenyl)-1,2-dimethyl-4-phenyl-1H-pyrrole-3-carboxylate (18)—**Ethyl acetoacetate (1.3 g, 10 mmol), benzaldehyde (1.06 g, 10 mmol), piperidine (43 μL), and acetic acid (128 μL) were dissolved in toluene (10 mL) and refluxed with azeotropic removal of water overnight. After the solution was cooled it was diluted with EtOAc, washed with 1.0 M HCl, saturated sodium bicarbonate, brine and dried over sodium sulfate. Removal of the solvent under vacuum gave a crude ethyl 2-benzylidene-3-oxobutanoate, which was used directly in the following step without further purification. To a solution of this compound, 4-chlorobenzaldehyde (1.41 g, 10mmol), and triethylamine (1.0 mL) was added 3-ethyl-5-(2-hydroxyethyl)-4-methylthiazolium bromide (0.38 g, 1.5mmol) and the mixture was stirred and heated at 70 °C overnight. After cooling to room temperature, the mixture was diluted with EtOAc, washed with 1M HCl, saturated sodium bicarbonate and brine then dried over sodium sulfate. The EtOAc was removed *in vacuo* and the residue was purified by flash chromatography on silica gel (1:5 ethyl acetate:hexane) to provide **17**, which was treated with methylamine in MeOH (2M, 8 mL) overnight. The reaction mixture was treated with 2M HCl (8 mL) for 20 min and extracted with EtOAc. The EtOAc solution was washed with brine, dried over sodium sulfate and concentrated *in vacuo*. The residue was purified by flash chromatography on silica gel (1:4 ethyl acetate:hexane) to give **18 (**2.45 g, 73% over three steps). $^1$H NMR (300 MHz, $CDCl_3$), δ 7.25 (d, J=8.4, 2H), 7.20~7.16 (m, 3H), 7.13~7.06 (m, 4H), 4.10 (q, J=7.1, 2H), 3.44 (s, 3H), 2.65 (s, 3H), 1.03 (t, J=7.1, 3H); $^{13}$C NMR (75 MHz, $CCl_3D$), δ 165.8, 136.2, 135.8, 133.4, 132.4, 130.8, 130.3, 130.2, 128.4, 127.2, 125.9, 124.1, 111.3, 59.2, 31.8, 13.9, 11.8; ESI MS: m/z 376.8 $(M + Na)^+$.

**5-(4-Chlorophenyl)-1,2-dimethyl-N-(3-(4-methylpiperazin-1-yl)propyl)-4-phenyl-1H-pyrrole-3-carboxamide (8)—**To a solution of ester **18** (0.53 g, 1.5 mmol) in a mixture of dioxane/ethanol/water (1:1:1, 12 mL) was added NaOH (0.3 g, 7.5mmol) and the solution was refluxed until starting material could no longer be observed by TLC. After cooling, the reaction was neutralized with 1M HCl and extracted with EtOAc. The EtOAc solution was washed with brine, dried over sodium sulfate and concentrated under vacuum to provide 5-(4-chlorophenyl)-1,2-dimethyl-4-phenyl-1H-pyrrole-3-carboxylic acid, which was used directly in the following step without further purification. A solution of this acid, 1-(3-aminopropyl)-4-methylpiperazine (0.35 g, 2.3 mmol), EDCI (0.44 g, 2.3mmol), HOBt

(0.30 g, 2.3 mmol) and N,N-diisopropylethylamine (0.54 mL, 3.0 mmol) in $CH_2Cl_2$ (10 mL) was stirred for 8 h then concentrated. The residue was purified by HPLC to afford **8** (0.62g, 89%).1H NMR (300 MHz, CD3OD), δ 7.21~7.10 (m, 5H), 7.03~7.00 (m, 4H), 3.49~3.45 (m, 4H), 3.39~3.35 (m, 4H), 3.34 (s, 3H), 3.21~3.19 (m, 2H), 2.91~2.89 (m, 2H), 2.87 (s, 3H), 2.38 (s, 3H), 1.78~1.73 (m, 2H);$^{13}$C NMR (75 MHz, CD3OD), δ 170.5, 136.6, 134.7, 133.7, 133.5, 131.9, 131.7, 131.2, 129.5, 129.2, 127.6, 122.7, 116.1, 55.3, 51.6, 43.4, 37.1, 32.0, 25.3, 11.4; ESI MS: m/z 465.8 $(M + H)^+$.

**Ethyl 5-(4-chlorophenyl)-4-(3-iodophenyl)-1,2-dimethyl-1*H*-pyrrole-3-carboxylate (20a)—**Ethyl acetoacetate (6.1 g, 47 mmol), 3-iodobenzaldehyde (10.8 g, 47 mmol), piperidine (200 μL), and acetic acid (600 μL) were dissolved in toluene (20 mL) and refluxed overnight with azeotropic removal of water. After the solution was cooled it was diluted with EtOAc, washed with 1.0 M HCl, saturated sodium bicarbonate, brine and dried over sodium sulfate. Removal of the solvent under vacuum gave a crude ethyl 2-(3-iodobenzylidene)-3-oxobutanoate, which was used directly in the following step without further purification. To a solution of this, ethyl 2-(3-iodobenzylidene)-3-oxobutanoate, 4-chlorobenzaldehyde (6.6 g, 47 mmol), and triethylamine (4.6 mL) was added 3-ethyl-5-(2-hydroxyethyl)-4-methylthiazolium bromide (1.9 g, 7.1 mmol) and the mixture was stirred and heated at 70 °C overnight. After cooling to room temperature, the mixture was diluted with EtOAc, washed with 1M HCl, saturated sodium bicarbonate, brine and dried over sodium sulfate. The EtOAc was removed *in vacuo* and the residue was purified by flash chromatography on silica gel (1:5 ethyl acetate:hexane) to give **19**, which was treated with a solution of methylamine in MeOH (2M, 35 mL) overnight. Then the reaction mixture was treated with 2M HCl (40 mL) for 20 min and extracted with EtOAc. The EtOAc solution was washed with brine, dried over sodium sulfate and concentrated *in vacuo*. The residue was purified by flash chromatography on silica gel (1:4 ethyl acetate:hexane) to afford **20a** (15.8 g, 70% over three steps). $^1$H NMR (300 MHz, $CCl_3D$), 7.54 (s, 1H), 7.49 (d, J=7.8, 1H), 7.28 (d, J=8.4, 2H), 6.99 (d, J=7.7, 1H), 6.89 (t, J=7.7, 1H), 4.10 (q, J=7.1, 2H), 3.43 (s, 3H), 2.64 (s, 3H), 1.06 (t, 7.1, 3H); $^{13}$C NMR (75 MHz, $CCl_3D$), δ 165.5, 139.9, 138.2, 136.7, 134.8, 133.8, 132.4, 130.4, 129.8, 128.9, 128.6, 122.3, 111.1, 93.0, 59.4, 31.8, 14.0, 11.8; ESI MS: *m*/*z* 480.3 $(M + H)^+$ .

**Ethyl 5-(4-chlorophenyl)-1-ethyl-4-(3-iodophenyl)-2-methyl-1H-pyrrole-3-carboxylate (20b)—**Intermediate **20b** was prepared from **19** in 86% yield by a procedure similar to that used for **20a**. $^1$H NMR (300 MHz, $CCl_3D$), δ 7.55 (s, 1H), 7.45 (d, J=7.7, 1H), 7.28 (d, J=7.9, 2H), 7.11 (d, J=7.9, 2H), 6.87 (t, J=7.7, 1H), 4.10 (q, J=7.1, 2H), 3.84 (q, J=7.1, 2H), 2.65 (s, 3H), 1.16 (t, J=7.0, 3H), 1.06 (t, J=7.1, 3H); $^{13}$C NMR (75 MHz, $CCl_3D$), δ 165.6, 139.9, 138.1, 135.7, 134.6, 134.0, 132.6, 130.2, 129.9, 129.8, 128.9, 128.6, 122.6, 111.2, 93.0, 59.3, 39.1, 16.1, 14.1, 11.5; ESI MS: *m*/*z* 494.0 $(M + H)^+$.

**Ethyl 5-(4-chlorophenyl)-4-(3-iodophenyl)-1-isopropyl-2-methyl-1H-pyrrole-3-carboxylate (20c)—**Ethyl 2-acetyl-4-(4-chlorophenyl)-3-(3-iodophenyl)-4-oxobutanoate **19** (5g, 10.3 mmol) in MeOH (30 mL) was added isopropyl amine (1.8 g, 31 mmol), acetic acid (5 mL). The reaction mixture was heated to 65 °C for 24 h in a sealed tube. Water (40 mL) was added and extracted with EtOAc (3 × 30 mL). The combined organic layers were washed with brine, dried over sodium sulfate and concentrated *in vacuo*. The residue was purified by flash chromatography on silica gel to provide **20c** (3.8g, 72%). $^1$H NMR (300 MHz, $CCl_3D$), δ 7.51 (s, 1H), 7.42 (d, J=7.8, 1H), 7.26 (d, J=8.1, 2H), 7.10 (d, J=7.9, 2H), 6.96 (d, J=7.2, 1H), 6.83 (t, J=7.7, 1H), 4.42~4.33 (m, 1H), 4.07 (q, J=7.1, 2H), 2.74 (s, 3H), 1.44 (d, J=7.0, 6H), 1.01 (t, J=7.1, 3H); $^{13}$C NMR (75 MHz, $CCl_3D$), δ 165.7, 139.8, 138.4, 135.5, 134.5, 134.0, 133.0, 131.0, 130.4, 129.6, 128.8, 128.5, 122.5, 112.2, 93.0, 59.3, 48.7, 22.3, 14.0, 13.1; ESI MS: *m*/*z* 508.4 $(M + H)^+$.

**Ethyl 5-(4-chlorophenyl)-1-cyclopropyl-4-(3-iodophenyl)-2-methyl-1H-pyrrole-3-carboxyl-ate (20d)—**Intermediate **20d** was prepared from **19** by a similar procedure as that for **20a** in 84% yield. $^1$H NMR (300 MHz, $CCl_3D$), δ 7.53~7.48 (m, 2H), 7.23 (d, J=8.5, 2H), 7.07 (d, J=8.5, 2H), 6.97 (d, J=7.7, 1H), 6.89 (t, 7.7, 1H), 4.08 (q, J=7.1, 2H), 3.15~3.09 (m, 1H), 2.71 (s, 3H), 1.04 (t, 7.1, 3H), 0.92~0.85 (m, 2H), 0.58~0.55 (m, 2H); $^{13}$C NMR (75 MHz, $CCl_3D$), δ 165.4, 140.0, 139.2, 138.3, 134.8, 133.0, 131.9, 131.1, 130.6, 129.9, 129.0, 128.1, 121.9, 111.4, 93.0, 59.3, 27.2, 14.0, 12.8, 9.6; ESI MS: *m*/*z* 506.6 $(M + H)^+$.

**5-(4-Chlorophenyl)-4-(3-iodophenyl)-1,2-dimethyl-1H-pyrrole-3-carboxylic acid (21a)—**Sodium hydroxide (4.2 g, 104mmol) was added to a solution of the ester **20a** (10 g, 20.8 mmol) in a mixture of dioxane/ethanol/water (1:1:1, 150 mL) and the solution was refluxed until no starting material was observed by TLC. After cooling the reaction was neutralized with 1M HCl and extracted with EtOAc. The EtOAc solution was washed with brine, dried over sodium sulfate and concentrated *in vacuo* to provide **21a** (9.4 g, 100% yield). $^1$H NMR (300 MHz, $CCl_3D$), 7.50~7.48 (m, 2H), 7.29 (d, J=8.3, 2H), 7.08~7.02 (m, 3H), 6.92 (t, J=8.0, 1H), 3.42 (s, 3H), 2.64 (s, 3H); $^{13}$C NMR (75 MHz, $CCl_3D$), δ 170.1, 139.7, 138.3, 137.5, 135.0, 133.9, 132.4, 131.0, 130.1, 129.7, 129.0, 128.6, 122.8, 109.7, 93.2, 32.0, 12.2; ESI MS: *m*/*z* 452.3 $(M + H)^+$.

**5-(4-Chlorophenyl)-1-ethyl-4-(3-iodophenyl)-2-methyl-1H-pyrrole-3-carboxylic acid (21b)—**Intermediate **21b** was prepared from **20b** in 97% yield using a similar procedure as that for **21a**. $^1$H NMR (300 MHz, $CCl_3D$) δ 7.51~7.45 (m, 2H), 7.31~7.28 (m, 2H), 7.10~7.05 (m, 3H), 6.90 (t, J=7.8, 1H), 3.83 (q, J=7.1, 2H), 2.65 (s, 3H), 1.17 (t, J=7.1, 3H); $^{13}$C NMR (75 MHz, $CCl_3D$), δ 169.9, 139.6, 137.4, 137.3, 134.9, 134.1, 132.6, 130.5, 130.0, 129.0, 128.6, 123.1, 109.9, 93.2, 39.2, 16.0, 11.9; ESI MS: *m*/*z* 466.3 $(M + H)^+$.

**5-(4-Chlorophenyl)-4-(3-iodophenyl)-1-isopropyl-2-methyl-1H-pyrrole-3-carboxylic acid (21c)—**Intermediate **21c** was prepared from **20c** in 98% yield using a similar procedure as that for **21a**. $^1$H NMR (300 MHz, $CCl_3D$) δ 7.46~7.43 (m, 2H), 7.30~7.27 (m, 2H), 7.08~7.02 (m, 3H), 6.88 (t, J=7.7, 1H), 4.41~4.32 (m, 1H), 2.73 (s, 3H), 1.44 (d, J=7.1, 6H); $^{13}$C NMR (75 MHz, $CCl_3D$) δ 169.0, 139.6, 137.7, 137.1, 134.8, 134.1, 133.0, 131.0, 130.7, 129.9, 128.9, 128.4, 123.0, 110.6, 93.1, 48.8, 13.4; ESI MS: *m*/*z* 502.5 $(M + Na)^+$.

**5-(4-Chlorophenyl)-1-cyclopropyl-4-(3-iodophenyl)-2-methyl-1H-pyrrole-3-carboxylic acid (21d)—**Intermediate **21d** was prepared in 98% yield from **20d** by a similar procedure as that for **21a**. $^1$H NMR (300 MHz, $CCl_3D$) δ 7.52~7.49 (m, 2H), 7.24 (d, J=8.5, 2H), 7.06~7.03 (m, 3H), 6.92 (t, J=7.7, 1H), 3.16~3.08 (m, 1H), 2.72 (s, 3H), 0.93~0.86 (m, 2H), 0.59~0.53 (m, 2H);$^{13}$C NMR (75 MHz, $CCl_3D$) δ 169.4, 140.8, 139.8, 137.5, 135.1, 133.1, 131.9, 131.7, 130.4, 130.1, 129.1, 128.2, 122.4, 109.9, 93.2, 27.3, 13.1, 9.6.

**5-(4-Chlorophenyl)-1,2-dimethyl-4-(3-(4-(4-nitrophenyl)piperazin-1-yl)phenyl)-1H-pyrrole-3-carboxylic acid (22a)—21a** (3.1g, 6.86 mmol), 1-(4-nitrophenyl)piperazine (2.84g, 13.7 mmol), CuI (131 mg, 0.69 mmol), L-proline (158 mg, 1.37mmol) and $K_2CO_3$ (1.89 g, 13.7mmol) were dissolved in DMSO (20 mL). This mixture was heated to 80 °C overnight under nitrogen. After the solution was cooled, saturated ammonium chloride solution was added and the solution was extracted with $CH_2Cl_2$. The combined organic layers were washed with brine and dried over sodium sulfate and concentrated. Purification of the residue by flash chromatography on silica gel (1:1 ethyl acetate:hexane) afforded **22a** (2.48 g, 68%). $^1$H NMR (300 MHz, $CCl_3D$) δ 8.13 (d, J=9.2,

2H), 7.28 (d, J=8.2, 2H), 7.08~7.06 (m, 3H), 6.84~6.78 (m, 4H), 6.68 (d, J=7.4, 1H), 3.50 (br. 4H), 3.44 (s, 3H), 3.18 (br. 4H), 2.63 (s, 3H); $^{13}$C NMR (75 MHz, $CCl_3D$), δ 170.0, 154.6, 138.6, 135.8, 133.7, 132.5, 130.9, 130.1, 128.6, 128.3, 126.0, 124.2, 120.2, 114.7, 112.7, 109.6, 49.3, 46.6, 32.0, 12.2; ESI MS: *m*/*z* 531.5 $(M + H)^+$.

**5-(4-Chlorophenyl)-1-ethyl-2-methyl-4-(3-(4-(4-nitrophenyl)piperazin-1-yl)phenyl)-1H-pyrrole-3-carboxylic acid (22b)—**Intermediate **22b** was prepared in 70% yield from **21b** using a similar procedure as that for **22a**. $^1$H NMR (300 MHz, $CCl_3D$) δ 8.13 (d. J=9.2, 2H), 7.28 (d, J=8.2, 2H), 7.12 (d, J=8.3, 2H), 7.05 (t, J=7.8, 1H), 6.83 (d, J=9.3, 2H), 6.73~6.66 (m, 3H), 3.85 (q, J=7.1, 2H), 3.46~3.45 (m, 4H), 3.17~3.15 (m, 4H), 2.64 (s, 3H), 1.18 (t, J=7.0, 3H); $^{13}$C NMR (75 MHz, $CCl_3D$), δ 170.8, 154.8, 149.4, 138.4, 137.1, 135.7, 133.8, 132.7, 130.6, 130.3, 128.6, 128.1, 126.0, 124.7, 123.2, 119.9, 114.2, 112.6, 109.9, 48.9, 46.7, 39.2, 16.0, 12.0; ESI MS: *m*/*z* 545.5 $(M + H)^+$.

**5-(4-Chlorophenyl)-1-isopropyl-2-methyl-4-(3-(4-(4-nitrophenyl)piperazin-1-yl)phenyl)-1H-pyrrole-3-carboxylic acid (22c)—**Intermediate **22c** was prepared from **21c** in 73% yield by a similar procedure as that for compound **22a**. $^1$H NMR (300 MHz, $CCl_3D$) δ 11.8 (br. 1H), 8.13 (d, J=9.1, 2H), 7.27 (d, J=8.6, 2H), 7.10 (d, J=8.2, 2H), 7.03 (t, J=8.2, 1H), 6.83 (d, J=9.2, 2H), 6.67~6.53 (m, 3H), 4.44~4.35 (m, 1H), 3.46 (br. 4H), 3.14 (br. 4H), 2.73 (s, 3H), 1.45 (d, J=7.0, 6H); $^{13}$C NMR (75 MHz, $CCl_3D$), δ 170.9, 154.8, 149.4, 138.4, 137.0, 136.0, 133.8, 133.1, 131.4, 130.8, 128.4, 128.0, 126.0, 124.6, 123.2, 119.8, 114.1, 112.6, 110.9, 48.9, 48.8, 46.7, 22.3, 13.5; ESI MS: *m*/*z* 559.6 $(M + H)^+$.

**5-(4-Chlorophenyl)-1-cyclopropyl-2-methyl-4-(3-(4-(4-nitrophenyl)piperazin-1-yl)phenyl)-1H-pyrrole-3-carboxylic acid (22d)—**Intermediate **22d** was prepared from **21d** in 76% yield by a similar procedure as that for compound **22a**. $^1$H NMR (300 MHz, $CCl_3D$) δ 8.13 (d, J=9.3, 2H), 7.22 (d, J=8.4, 2H), 7.12~7.05 (m, 3H), 6.83 (d, J=8.4, 2H), 6.74~6.70 (m, 2H), 6.64 (d, J=7.5, 1H), 3.48~3.45 (m, 4H), 3.18~3.15 (m, 5H), 2.70 (s, 3H), 0.93~0.86 (m, 2H), 0.56~0.53 (m, 2H); $^{13}$C NMR (75 MHz, $CCl_3D$), δ 170.2, 154.8, 149.6, 140.6, 138.4, 135.8, 132.9, 132.0, 131.5, 131.0, 128.2, 128.1, 125.9, 123.9, 123.3, 120.0, 114.4, 112.6, 110.1, 48.9, 46.7, 27.3, 13.2, 9.7; ESI MS: *m*/*z* 557.9 $(M + H)^+$.

**5-(4-Chlorophenyl)-4-(3-(4-(4-(4-fluoro-3-nitrophenylsulfonamido)phenyl)piperazin-1-yl)phenyl)-1,2-dimethyl-1H-pyrrole-3-carboxylic acid (23a)—**To a solution of compound **22a** (1.2 g, 2.3 mmol) in a mixture of $CH_2Cl_2$ (10 mL) and MeOH (10 mL) was added 10% Pd-C (120 mg). The solution was stirred under 1 atm of $H_2$ at room temperature for 0.5 hour before filtering through celite and being concentrated. The resulting aniline was used in the next step without purification. To this aniline in pyridine (20 mL), 4-fluoro-3-nitrobenzene-1-sulfonyl chloride (0.54 g, 2.3 mmol) was added at 0 °C. The mixture was stirred at 0 °C for 30 minutes. The pyridine was removed under vacuum and the residue was purified by flash chromatography on silica gel (3:2 ethyl acetate:hexane) to give **23a** (1.18 g, 74% in two steps). $^1$H NMR (300 MHz, $CCl_3D$) δ 8.43 (dd, J=2.1, 6.7, 1H), 7.89~7.86 (m, 1H), 7.33 (d, J=9.6, 1H), 7.25 (d, J=8.4, 2H), 7.16 (br. 1H), 7.08~7.05 (m, 3H), 6.80 (d, J=8.9, 2H), 6.73 (s, 2H), 6.66 (d, J=7.4, 1H), 3.44 (s, 3H), 3.17~3.11 (m, 8H), 2.64 (s, 3H); $^{13}$C NMR (75 MHz, $CCl_3D$:$CD_3OD$=5:1), δ 167.7, 149.8, 149.5, 137.0, 136.7, 136.6, 135.9, 134.2, 134.1, 133.3, 132.3, 130.4, 130.3, 128.3, 127.9, 127.5, 125.6, 124.6, 124.1, 123.3, 119.7, 119.3, 119.0, 116.7, 114.5, 110.2, 49.7, 48.1, 31.7, 11.8;ESI MS: *m*/*z* 704.6 $(M + H)^+$.

**5-(4-Chlorophenyl)-1-ethyl-4-(3-(4-(4-(4-fluoro-3-nitrophenylsulfonamido)phenyl)-piperazin-1-yl)phenyl)-2-methyl-1H-pyrrole-3-carboxylic acid (23b)—**Intermediate **23b** was prepared from **22b** in 67% yield in two

steps using a similar procedure as that for **23a**. $^1$H NMR (300 MHz, $CCl_3D$) δ 8.44 (dd, J=2.2, 6.8, 1H), 7.89~7.86 (m, 1H), 7.34~7.25 (m, 3H), 7.11 (d, J=8.4, 2H), 7.04 (t, J=8.0, 1H), 6.95 (d, J=8.9, 2H), 6.80 (d, J=8.9, 2H), 6.72~6.64 (m, 3H), 3.85 (q, J=7.1, 2H), 3.18~3.10 (m, 8H), 2.65 (s, 3H), 1.18 (t, J=7.1, 3H); $^{13}$C NMR (75 MHz, $CCl_3D$), δ 169.8, 150.1, 149.9, 137.14, 137.07, 136.4, 135.7, 134.4, 134.3, 133.8, 132.7, 130.6, 130.3, 128.5, 128.1, 126.5, 125.9, 125.5, 124.7, 123.1, 119.8, 119.6, 119.3, 116.6, 114.4, 109.8, 49.3, 48.7, 39.2, 16.0, 12.0; ESI MS: *m*/*z* 740.3 $(M + Na)^+$.

**5-(4-Chlorophenyl)-4-(3-(4-(4-(4-fluoro-3-nitrophenylsulfonamido)phenyl)piperazin-1-yl)phenyl)-1-isopropyl-2-methyl-1H-pyrrole-3-carboxylic acid (23c)—**Intermediate **23c** was prepared in 71% yield in two steps using a similar procedure as that for **23a**. $^1$H NMR (300 MHz, $CCl_3D$) δ 8.45 (dd, J=2.1, 6.7, 1H), 7.90~7.85 (m, 1H), 7.39 (br., 1H), 7.34~7.23 (m, 3H), 7.10~7.01 (m, 3H), 6.95 (d, J=8.8, 2H), 6.81 (d, J=8.9, 2H), 6.71~6.63 (m, 3H), 4.43~4.34 (m, 1H), 3.18~3.10 (m, 8H), 2.73 (s, 3H), 1.45 (d, J=7.0, 6H); $^{13}$C NMR (75 MHz, $CCl_3D$), δ 169.7, 150.1, 149.9, 137.2, 137.0, 136.9, 136.5, 136.4, 135.9, 134.4, 134.3, 133.8, 133.1, 131.3, 130.8, 128.3, 128.1, 126.5, 125.9, 125.5, 124.6, 123.1, 119.6, 119.3, 116.6, 114.4, 110.8, 49.3, 48.8, 48.7, 22.2, 13.5; ESI MS: *m*/*z* 754.2 $(M + Na)^+$.

**(R)-5-(4-Chlorophenyl)-4-(3-(4-(4-(4-((4-(dimethylamino)-1-(phenylthio)butan-2-yl)amino)-3-nitrophenylsulfonamido)phenyl)piperazin-1-yl)phenyl)-1,2-dimethyl-1H-pyrrole-3-carboxylic acid (12)—**DIEA (70 μL, 0.4 mmol) was added to a solution of **23a** (158 mg, 0.22mmol) and (*R*)-$N^1$,$N^1$-dimethyl-4-phenylthio)butane-1,3-diamine (51 mg, 0.22mmol) in DMF. The solution was stirred overnight and concentrated. The residue was purified by HPLC to afford **12** (145 mg, 71%). $^1$H NMR (300 MHz, $CD_3OD$), δ 8.30 (d, J=2.2 Hz, 1H), 7.59 (dd, J=2.2, 9.2, 1H), 7.26~7.23 (m, 2H), 7.18~7.13 (m, 3H), 7.09~6.88 (m, 13H), 4.10~4.07 (m, 1H), 3.40 (s, 3H), 3.36-3.29 (m, 9H), 3.21-3.15(m, 3H), 2.83 (s, 6H), 2.58 (s, 3H), 2.26-2.10 (m, 2H); $^{13}$C NMR (75 MHz, $CD_3OD$), δ 169.1, 148.5, 148.0, 146.9, 139.0, 138.4, 136.2, 134.8, 134.4, 134.0, 132.3, 132.2, 132.1, 131.9, 131.6, 130.1, 129.6, 129.5, 129.0, 128.0, 127.9, 127.6, 124.8. 124.3, 122.9, 118.9, 117.2, 116.2, 111.5, 55.9, 53.2, 52.4, 50.1, 43.5, 39.5, 32.2, 30.1, 12.1; ESI MS: *m*/*z* 908.9 $(M + H)^+$.

**(R)-5-(4-Chlorophenyl)-4-(3-(4-(4-(4-((4-(dimethylamino)-1-(phenylthio)butan-2-yl)amino)-3-nitrophenylsulfonamido)phenyl)piperazin-1-yl)phenyl)-1-ethyl-2-methyl-1H-pyrrole-3-carboxylic acid (14)—**Compound **14** was prepared from **23b** in 81% yield using a similar procedure as that for compound **12**. $^1$H NMR (300 MHz, $CD_3OD$) δ 8.24 (d, J=2.1, 1H), 7.54 (dd, J=2.1, 9.1, 1H), 7.20 (d, J=8.4, 2H), 7.12~6.85 (m, 16H), 4.06~4.03 (m, 1H), 3.80 (q, J=7.1, 2H), 3.28~3.24 (m, 9H), 3.16~3.09 (m, 3H), 2.78 (s, 6H), 2.54 (s, 3H), 2.22~2.06 (m, 2H), 1.03 (t, J=7.1, 3H); $^{13}$C NMR (75 MHz, $CD_3OD$), δ 169.1, 148.1, 148.0, 145.9, 139.1, 137.4, 136.2, 135.1, 134.4, 134.3, 132.6, 132.1, 132.0, 131.7, 131.6, 130.1, 129.64, 129.58, 128.0, 127.9, 127.4, 125.1, 124.1, 123.1, 119.0, 117.5, 116.4, 111.7, 55.9, 53.6, 52.4, 50.0, 43.5, 40.2, 39.5, 30.1, 16.2, 12.0; ESI MS: *m*/*z* 922.6 $(M + H)^+$.

**(*R*)-5-(4-Chlorophenyl)-4-(3-(4-(4-(4-((4-(dimethylamino)-1-(phenylthio)butan-2-yl)amino)-3-nitrophenylsulfonamido)phenyl)piperazin-1-yl)phenyl)-1-isopropyl-2-methyl-1H-pyrrole-3-carboxylic acid (15)—**Compound **15** was prepared from **22c** in 79% yield using a similar procedure as that for **12**. $^1$H NMR (300 MHz, $CD_3OD$), δ 8.29 (d, J=2.2, 1H), 7.60 (dd, J=2.2, 9.2, 1H), 7.26~6.90 (m, 18H), 4.41~4.36 (m, 1H), 4.10~4.08 (m, 1H), 3.38~3.31 (m, 9H), 3.21~3.15 (m, 3H), 2.83 (s, 6H), 2.68 (s, 3H), 2.24~2.14 (m, 2H), 1.39 (d, J=7.1, 6H); $^{13}$C NMR (75 MHz, $CD_3OD$), δ 169.2, 148.2,

148.0, 145.8, 139.4, 137.1, 136.2, 135.2, 134.8, 134.4, 132.9, 132.6, 132.2, 132.1, 131.6, 130.1, 129.9, 129.6, 129.4, 128.0, 127.9, 127.6, 125.1. 124.2, 122.9, 119.0, 117.5, 116.2, 112.8, 55.9, 53.8, 52.4, 50.3, 50.0, 43.5, 39.5, 30.1, 22.5, 13.5; ESI MS: *m*/*z* 936.8 $(M + H)^+$.

**(*R*)-5-(4-Chlorophenyl)-1-cyclopropyl-4-(3-(4-(4-(4-((4-(dimethylamino)-1-(phenylthio)-butan-2-yl)amino)-3-nitrophenylsulfonamido)phenyl)piperazin-1-yl)phenyl)-2-methyl-1H-pyrrole-3-carboxylic acid (16)—**Compound **16** was prepared from **22d** in 78% yield by a similar procedure as that for compound **12**. $^1$H NMR (300 MHz, $CD_3OD$), δ 8.29 (d, J=2.3, 1H), 7.60 (dd, J=2.3, 9.2, 1H), 7.24~6.91 (m, 18H), 4.12~4.07 (m, 1H), 3.39~3.31 (m, 9H), 3.24~3.14 (m, 4H), 2.83 (s, 6H), 2.67 (s, 3H), 2.24~2.15 (m, 2H), 0.89~0.82 (m, 2H), 0.50~0.44 (m, 2H); $^{13}$C NMR (75 MHz, $CD_3OD$), δ 169.0, 148.5, 147.9, 140.8, 139.0, 136.2, 134.4, 134.1, 133.6, 132.8, 132.7, 132.3, 131.6, 130.1, 129.6, 129.1, 128.0, 127.9, 127.7, 124.5, 124.3, 122.9, 118.9, 117.3, 116.2, 112.0, 55.9, 53.2, 52.4, 50.1, 43.5, 39.6, 30.1, 28.3, 13.2, 10.3; ESI MS: *m*/*z* 935.3 $(M + H)^+$.

**5-(4-Chlorophenyl)-4-(3-iodophenyl)-1,2-dimethyl-N-(3-(4-methylpiperazin-1-yl)propyl)-1H-pyrrole-3-carboxamide (24)—**A solution of **21a** (1.0 g, 2.2 mmol), 1-(3-aminopropyl)-4-methylpiperazine (0.52g, 3.3 mmol), EDCI (0.64g, 3.3mmol), HOBt (0.43 g, 3.3 mmol) and N,N-diisopropylethylamine (0.77 mL, 4.4 mmol) in $CH_2Cl_2$ (15 mL) was stirred for 8 h then concentrated. The residue was purified by flash chromatography on silica gel (2:1 ethyl acetate:methanol) to afford **24** (1.1 g, 86%).$^1$H NMR (300 MHz, $CCl_3D$), δ7.42 (s, 1H), 7.39 (d, J=7.9, 1H), 7.16 (d, d, J=8.4, 2H), 6.95~6.92 (m, 3H), 6.82 (t, J=7.7, 1H), 5.41 (t, J=5.3, 1H), 3.28 (s, 3H), 3.19~3.11 (m, 2H), 2.44 (s, 3H), 2.24~2.11 (m, 11H), 2.04 (t, J=7.0, 2H), 1.43~1.34 (m, 2H); $^{13}$C NMR (75 MHz, $CCl_3D$), δ165.7, 139.3, 137.1, 135.4, 133.7, 133.4, 132.2, 129.9, 129.8, 129.6, 128.6, 119.0, 115.1, 94.1, 55.9, 55.0, 53.0, 46.0, 37.9, 31.6, 26.3, 11.3; ESI MS: *m*/*z* 591.7 $(M + H)^+$.

**(R)-5-(4-Chlorophenyl)-4-(3-(4-(4-(((4-((4-(dimethylamino)-1-(phenylthio)butan-2-yl)amino)phenyl)sulfonyl)carbamoyl)phenyl)piperazin-1-yl)phenyl)-1,2-dimethyl-N-(3-(4-methylpiperazin-1-yl)propyl)-1H-pyrrole-3-carboxamide (9)—**$Pd(dba)_2$ (3.5 mg, 0.006 mmol), tri-*tert*-butylphosphine in toluene (1M, 4.8 μL), and sodium *tert*-butoxide (18 mg, 0.18 mmol) were added to a stirred slurry of **24** (71mg, 0.12 mmol) and **25** (88 mg, 0.14 mmol) in a mixture of toluene/DMF (1:1, 4 mL) at room temperature under nitrogen. The mixture was heated to 70 °C and monitored by thin-layer chromatography. After complete consumption of starting materials, the reaction mixture was filtered through celite and concentrated. Purification of the residue by HPLC yielded **9** (37 mg, 29%). $^1$H NMR (300 MHz, $CD_3OD$), δ 8.59 (d, J=2.3, 1H), 7.83 (dd, J=2.3, 9.2, 1H), 7.68 (d, d, J=8.9, 2H), 7.21~7.06 (m, 5H), 7.03~6.84 (m, 9H), 6.75~6.74 (m, 2H), 4.09~4.08 (m, 1H), 3.50~3.25 (m, 16H), 3.20~3.14 (m, 9H), 2.95~2.79 (m, 11H), 2.34 (s, 3H), 2.20~2.12 (m, 2H), 1.82~1.77 (m, 2H);$^{13}$C NMR (75 MHz, $CD_3OD$), δ 170.3, 167.1, 155.5, 148.5, 137.8, 136.2, 135.4, 134.8, 133.9, 133.4, 132.1, 132.0, 131.5, 131.3, 130.4, 130.2, 130.1, 129.8, 129.6, 127.9, 127.3, 122.5, 121.9, 120.7, 119.8, 116.7, 116.2, 116.0, 115.055.9, 55.4, 52.5, 52.3, 51.7, 47.6, 43.6, 43.5, 39.3, 37.3, 32.1, 30.1, 25.4, 11.5; ESI MS: *m*/*z* 1076.3 $(M + H)^+$ .

**(R)-5-(4-Chlorophenyl)-4-(3-(4-(4-(4-((4-(dimethylamino)-1-(phenylthio)butan-2-yl)amino)-3-nitrophenylsulfonamido)phenyl)piperazin-1-yl)phenyl)-1,2-dimethyl-N-(3-(4-methylpiperazin-1-yl)propyl)-1H-pyrrole-3-carboxamide (10)—**A mixture of **12** (88 mg, 0.097mmol), 1-(3-aminopropyl)-4-methylpiperazine (22.8 mg, 0.145 mmol), EDCI (27.9 mg, 0.145 mmol), HOBt (18.7 mg, 0.145 mol) and DIEA (52 μL, 0.29 mmol) in $CH_2Cl_2$ (5 mL) was stirred for 8 h and concentrated. The residue was purified

by HPLC to provide **10** (86 mg, 85%). $^1$H NMR (300 MHz, $CD_3OD$), δ 8.29 (d, J=2.1, 1H), 7.58 (dd, J=2.1, 9.0, 1H), 7.26 (d, J=8.3, 2H), 7.17~6.89 (m, 14H), 6.73~6.70 (m, 2H), 4.10~4.05 (m, 1H), 3.38~3.31 (m, 10H), 3.24~3.18 (m, 15H), 2.82~2.87 (m, 11H), 2.42 (s, 3H), 2.20~2.16 (m, 2H), 1.76~1.71 (m, 2H); $^{13}$C NMR (75 MHz, $CD_3OD$), δ 170.3, 150.3, 148.5, 148.0, 137.7, 136.2, 134.8, 134.4, 133.8, 133.3, 132.5, 132.2, 132.1, 131.6, 131.2, 130.2, 130.1, 129.6, 128.0, 127.9, 127.6, 125.1, 124.2, 122.6, 120.6, 118.9, 116.3, 116.2, 55.9, 55.3, 52.6, 52.4, 51.1, 50.9, 50.4, 43.6, 43.5, 39.5, 37.4, 32.0, 30.1, 25.9, 11.4; ESI MS: $m/z$ 1047.8$(M + H)^+$.

**(R)-5-(4-Chlorophenyl)-4-(3-(4-(4-(4-((4-(dimethylamino)-1-(phenylthio)butan-2-yl)amino)-3-nitrophenylsulfonamido)phenyl)piperazin-1-yl)phenyl)-N,1,2-trimethyl-1H-pyrrole-3-carboxamide (11)—**A mixture of **12** (37 mg, 0.039 mmol), methylamine in THF (2M, 39 μM, 0.078 mmol), EDCI (15.0 mg, 0.078 mmol), HOBt (10.1mg, 0.078mol) and DIEA (22 μL, 0.12 mmol) in $CH_2Cl_2$ (3 mL) was stirred for 8 h then concentrated. The residue was purified by HPLC to provide **11** (30 mg, 81%). $^1$H NMR (300 MHz, $CD_3OD$), δ 8.36 (d, J=2.1, 1H), 7.65 (dd, J=2.1, 9.2, 1H), 7.33 (d, J=8.4, 2H), 7.35~7.01 (m, 13H), 6.97 (d, J=9.2, 1H), 6.91 (s, 1H), 6.85 (d, J=7.4, 1H), 4.15~4.14 (m, 1H), 3.43~3.36 (m, 12H), 3.27~3.20 (m, 3H), 2.89 (s, 6H), 2.73 (s, 3H), 2.45 (s, 3H), 2.30~2.15 (m, 2H); $^{13}$C NMR (75 MHz, $CD_3OD$), δ 170.2, 148.3, 147.9, 147.5, 137.8, 136.2, 134.8, 134.4, 133.9, 133.2, 132.9, 132.24, 132.16, 131.6, 131.1, 130.3, 130.1, 129.6, 128.0, 127.9, 127.6, 126.9, 124.1, 121.9, 121.2, 119.3, 117.0, 116.7, 116.2, 55.9, 52.4, 52.3, 50.8, 43.5, 39.5, 31.9, 30.1, 26.6, 11.3; ESI MS: $m/z$ 921.3 $(M + H)^+$.

**(R)-N-(4-(4-(3-(2-(4-Chlorophenyl)-1,5-dimethyl-1H-pyrrol-3-yl)phenyl)piperazin-1-yl)phenyl)-4-((4-(dimethylamino)-1-(phenylthio)butan-2-yl)amino)-3-nitrobenzenesulfonamide (13)—**TFA (0.5 mL) was added to a solution of **12** (45mg, 0.050 mmol) in $CH_2Cl_2$ (2 mL). The solution was stirred for 15 min and evaporated. The residue was purified by HPLC to afford compound **13** (38 mg, 88%). $^1$H NMR (300 MHz, $CD_3OD$), δ 8.28 (d, J=2.2, 1H), 7.59 (dd, J=2.2, 9.1, 1H), 7.34 (d, J=8.4, 2H), 7.18~6.89 (m, 17H), 4.09~4.05 (m, 1H), 3.36~3.27 (m, 1H), 3.20~3.14 (m, 4H), 2.82 (s, 6H), 2.24 (s, 3H), 2.16~2.14 (m, 2H); $^{13}$C NMR (75 MHz, $CD_3OD$), δ 148.02, 148.95, 147.2, 140.1, 136.2, 134.7, 134.4, 134.0, 133.7, 132.7, 132.2, 131.6, 131.2, 130.6, 130.1, 130.0, 128.0, 127.9, 127.5, 125.5, 124.1, 122.0, 119.0, 118.9, 116.2, 55.9, 53.2, 52.4, 50.2, 43.5, 39.5, 31.6, 30.1, 12.4; ESI MS: $m/z$ 865.3 $(M + H)^+$.

## Fluorescence polarization-based (FP) binding assays

The expression and purification of Bcl-2, Bcl-xL and Mcl-1 proteins and the FP binding assay methods are the same as previously described.[17] Briefly, $IC_{50}$ and $K_i$ values of our synthesized compounds to Bcl-2/Bcl-xL/Mcl-1 proteins were determined in competitive binding experiments. Mixtures of serial dilutions of tested compounds and pre-incubated protein/probe complex were incubated at room temperature for 1–2 hours with gentle shaking. The final concentrations of proteins and fluorescent probes were 1.5 nM and 1 nM for the Bcl-2 assay, 10 nM and 2 nM for the Bcl-xL assay, and 20 nM and 2 nM for the Mcl-1 assay, respectively. Final DMSO concentration is 4%. Fluorescence polarization (mP) values were measured and plotted over total compound concentrations. $IC_{50}$ values were determined by nonlinear regression fitting of the binding curves. $K_i$ values were calculated as described previously.[22]

## Molecular modeling

Crystal structures of Bcl-xL with **1**[24] (PDB entry: 2YXJ) and **7** were used to model the binding stances of our designed compounds with Bcl-xL with the GOLD program (version 4.0.1).[25, 26] In the docking simulation, the center of the binding sites for Bcl-xL was set at

F97 and the radius of the binding site was defined as 12 Å, large enough to cover all the binding pockets. For each genetic algorithm (GA) run, a maximum of 200,000 operations were performed on a population of 5 islands of 100 individuals. Operator weights for crossover, mutation and migration were set to 95, 95 and 10 respectively. The docking simulation was terminated after 20 runs for **8** and designed compounds. ChemScore, implemented in Gold, was used as the fitness function to evaluate the docked conformations. The 20 conformations ranked highest by each fitness function were saved for analysis of the predicted docking modes. All the ligand modifications were performed using the Sybyl program.[27]

### Cell-free mitochondrial functional assays

The MDA-MB-231 (subclone 2LMP) cancer cell line was used in the functional assays. Cells were cultured in 150 mm cell culture dishes up to 80% confluent in a healthy state. After harvesting, cell pellets were washed by cold PBS.

Cell pellets were reconstituted in the mitochondrial isolation buffer (MIB, 10mM Tris, 0.1mM EDTA, 250mM sucrose with protease inhibitors and 1mM PMSF added immediately prior to the assay, pH = 7.4). Mixtures were incubated at 4 °C for 20 min with occasional gentle shaking. Following homogenizing the cells with glass cell homogenizer on ice, mitochondria were isolated by differential centrifugation steps followed by two washes in MIB and the third wash in mitochondrial reaction buffer (MRB, 20mM HEPES, 100mM KCl, 2.5mM $MgCl_2$, 100mM sucrose, 1mM DTT, with protease inhibitors and 1mM PMSF added immediately prior to the assay, pH = 7.5).

Enriched mitochondria pellets were resuspended in the mitochondria resuspending buffer. Aliquots of the mitochondria suspensions (total protein 100–150μg for each aliquot) were incubated with Bcl-2 or Bcl-xL or Mcl-1 protein, together with BIM peptide, and different concentrations of an inhibitor at 37 °C for 1 h. Mitochondria treated with DMSO were included as the negative control. Cytochrome *c* and Smac released to the supernatant and remaining in the mitochondria pellets were analyzed by Western Blotting using primary anti-Cytochrome *c* and anti-Smac antibodies from Cell Signaling (Danvers, MA) and Calbiochem (Darmstadt, Germany), respectively. The results were shown in Figure 4.

### Assays of cell growth and cell death and Western blotting

These assays were performed same as previously described.[17] Human small cell lung cancer cell lines H146 and H1417 were purchased from American Type Culture Collection (ATCC) and were maintained in RPMI-1640 medium containing 10% FBS. Rabbit antibodies against PARP and caspase-3 are from Cell Signaling Technology. Rabbit anti-GAPDH is from Santa Cruz Biotechnology.

### Assay to assess release of cytochrome C from mitochondria in cells

To examine release of cytochrome C from mitochondria into cytosol, H146 cancer cells were treated with different concentrations of compounds **14** and **15** for 2 h. Cells were collected. Release of cytochrome C from mitochondria into cytosol was analyzed using the Cytochrome C Assay kit (Millipore).

### *In vivo* pharmacodynamic (PD) and efficacy studies in the H146 xenograft model

For *in vivo* PD and efficacy studies, the H146 small-cell lung cancer xenograft model was employed. To develop xenograft tumors, $5 \times 10^6$ H146 cancer cells with matrigel were injected subcutaneously on the dorsal side of the SCID mice (from Charles River), one tumor per mouse.

For PD studies, mice bearing H146 xenograft tumors were administered with a single dose of **14**, **1** or vehicle when tumor volume was approximately 100 $mm^3$. Tumor tissues were harvested at indicated time points. Tumor tissues were analyzed using Western blotting to examine levels of PARP and caspase-3, as well as cleaved PARP and caspase-3 in the tumor tissues.

For efficacy studies, when tumors reached tumor volumes between 40–110 $mm^3$, mice were randomized into different groups, 8 mice per group, with a mean tumor volume of 70 $mm^3$. Mice were treated with **14** at 25 mg/kg, intravenously, daily, 5 days a week for 2 weeks, or **1** at 100 mg/kg, intraperitoneally, daily, 5 days a week for 2 weeks, or vehicle control. Tumor sizes and animal weights were measured 3 times a week during the treatment and twice a week after the treatment. Data are presented as mean tumor volumes ± SEM. Statistical analyses were performed by two-way ANOVA and unpaired two-tailed t test, using Prism (version 4.0, GraphPad, La Jolla, CA). $P < 0.05$ was considered statistically significant. The efficacy experiment was performed under the guidelines of the University of Michigan Committee for Use and Care of Animals.

### Bcl-xL Crystallographic studies

Expression and Purification of Bcl-xL protein was used the same method as described earlier.[17] Prior to crystallization, Bcl-xL was incubated with a 5-fold molar excess of compound **12** in the presence of 4% DMSO for 1 h at 4 °C and then concentrated to 7 mg/mL. Crystals of Bcl-xL:**12** were grown by vapor diffusion in a sitting drop tray against a well solution of 4% PEG 3000, 0.6 M zinc acetate, and 100 mM sodium acetate pH 4.5. In each experiment, the crystallization drops contained equal volumes of protein and well solution. Prior to data collection, crystals were cryoprotected in well solution with increasing amounts of glycerol to a final concentration of 20%, then flash frozen in liquid nitrogen.

X-ray data was collected at LS-CAT ID-21-F and G lines at the Advanced Photon Source at Argonne National Lab. Data were processed with HKL2000.[28] Bcl-xL:**12** crystallized in $P2_12_12_1$ space group and diffracted to 1.4 Å resolution. The structure contained one molecule in the asymmetric unit. The structure of the complex was solved by molecular replacement with Phaser[29] using a structure of Bcl-xL previously solved in our laboratory as a starting model. Iterative rounds of refinement and model building were completed using Buster[30] and Coot[31] respectively. The initial Fo-Fc electron density map revealed the presence of the compounds in the binding site of Bcl-xL. Every atom of **12** was visible in the Fo-Fc electron density map contoured at 3 sigma. The PRODRG server[32] was used to create the starting coordinates and restraint files for the compounds. The current Rfree/Rwork for the Bcl-xL:**12** structure is 0.1847/.0.1641. All amino acids fall into the allowed regions of the Ramanchandran plot with 98% in the preferred regions. Data collection and refinement statistics are given in Table S1 in SI.

## Supplementary Material

Refer to Web version on PubMed Central for supplementary material.

## Acknowledgments

This research was supported in part by a grant from the National Cancer Institute, National Institutes of Health (U19CA113317). Use of the Advanced Photon Source was supported by the U. S. Department of Energy, Office of Science, Office of Basic Energy Sciences, under Contract No. DE-AC02-06CH11357. Use of the LS-CAT Sector 21 was supported by the Michigan Economic Development Corporation and the Michigan Technology Tri-Corridor for the support of this research program (Grant 085P1000817). Coordinates for Bcl-xL complexed with **12** were deposited into the Protein Data Bank with accession numbers 3SP7.

## References


1. Hanahan D, Weinberg RA. Hallmarks of cancer: the next generation. Cell. 2011; 144:646–674. [PubMed: 21376230]
2. Adams JM, Cory S. The Bcl-2 apoptotic switch in cancer development and therapy. Oncogene. 2007; 26:1324–1337. [PubMed: 17322918]
3. Lowe SW, Cepero E, Evan G. Intrinsic tumour suppression. Nature. 2004; 432:307–315. [PubMed: 15549092]
4. Evan G, Littlewood T. A matter of life and cell death. Science. 1998; 281:1317–1322. [PubMed: 9721090]
5. Ziegler DS, Kung AL. Therapeutic targeting of apoptosis pathways in cancer. Curr Opin Oncol. 2008; 20:97–103. [PubMed: 18043263]
6. Reed JC. Apoptosis-based therapies. Nat Rev Drug Discov. 2002; 1:111–121. [PubMed: 12120092]
7. Cory S, Adams JM. The Bcl2 family: regulators of the cellular life-or-death switch. Nat Rev Cancer. 2002; 2:647–656. [PubMed: 12209154]
8. Cory S, Adams JM. Killing cancer cells by flipping the Bcl-2/Bax switch. Cancer Cell. 2005; 8:5–6. [PubMed: 16023593]
9. Labi V, Erlacher M, Kiessling S, Villunger A. BH3-only proteins in cell death initiation, malignant disease and anticancer therapy. Cell Death Differ. 2006; 13:1325–1338. [PubMed: 16645634]
10. Lessene G, Czabotar PE, Colman PM. BCL-2 family antagonists for cancer therapy. Nat Rev Drug Discov. 2008; 7:989–1000. [PubMed: 19043450]
11. Oltersdorf T, Elmore SW, Shoemaker AR, Armstrong RC, Augeri DJ, Belli BA, Bruncko M, Deckwerth TL, Dinges J, Hajduk PJ, Joseph MK, Kitada S, Korsmeyer SJ, Kunzer AR, Letai A, Li C, Mitten MJ, Nettesheim DG, Ng S, Nimmer PM, O'Connor JM, Oleksijew A, Petros AM, Reed JC, Shen W, Tahir SK, Thompson CB, Tomaselli KJ, Wang B, Wendt MD, Zhang H, Fesik SW, Rosenberg SH. An inhibitor of Bcl-2 family proteins induces regression of solid tumours. Nature. 2005; 435:677–681. [PubMed: 15902208]
12. Petros AM, Dinges J, Augeri DJ, Baumeister SA, Betebenner DA, Bures MG, Elmore SW, Hajduk PJ, Joseph MK, Landis SK, Nettesheim DG, Rosenberg SH, Shen W, Thomas S, Wang X, Zanze I, Zhang H, Fesik SW. Discovery of a potent inhibitor of the antiapoptotic protein Bcl-xL from NMR and parallel synthesis. J Med Chem. 2006; 49:656–663. [PubMed: 16420051]
13. Wendt MD, Shen W, Kunzer A, McClellan WJ, Bruncko M, Oost TK, Ding H, Joseph MK, Zhang H, Nimmer PM, Ng SC, Shoemaker AR, Petros AM, Oleksijew A, Marsh K, Bauch J, Oltersdorf T, Belli BA, Martineau D, Fesik SW, Rosenberg SH, Elmore SW. Discovery and structure-activity relationship of antagonists of B-cell lymphoma 2 family proteins with chemopotentiation activity in vitro and in vivo. J Med Chem. 2006; 49:1165–1181. [PubMed: 16451081]
14. Park CM, Bruncko M, Adickes J, Bauch J, Ding H, Kunzer A, Marsh KC, Nimmer P, Shoemaker AR, Song X, Tahir SK, Tse C, Wang X, Wendt MD, Yang X, Zhang H, Fesik SW, Rosenberg SH, Elmore SW. Discovery of an orally bioavailable small molecule inhibitor of prosurvival B-cell lymphoma 2 proteins. J Med Chem. 2008; 51:6902–6915. [PubMed: 18841882]
15. Tse C, Shoemaker AR, Adickes J, Anderson MG, Chen J, Jin S, Johnson EF, Marsh KC, Mitten MJ, Nimmer P, Roberts L, Tahir SK, Xiao Y, Yang X, Zhang H, Fesik S, Rosenberg SH, Elmore SW. ABT-263: a potent and orally bioavailable Bcl-2 family inhibitor. Cancer Res. 2008; 68:3421–3428. [PubMed: 18451170]
16. Sleebs BE, Czabotar PE, Fairbrother WJ, Fairlie WD, Flygare JA, Huang DC, Kersten WJ, Koehler MF, Lessene G, Lowes K, Parisot JP, Smith BJ, Smith ML, Souers AJ, Street IP, Yang H, Baell JB. Quinazoline sulfonamides as dual binders of the proteins B-cell lymphoma 2 and B-cell lymphoma extra long with potent proapoptotic cell-based activity. J Med Chem. 2011; 54:1914–1926. [PubMed: 21366295]
17. Zhou H, Chen J, Meagher JL, Yang CY, Aguilar A, Liu L, Bai L, Cong X, Cai Q, Fang X, Stuckey JA, Wang S. Design of Bcl-2 and Bcl-xL Inhibitors with Subnanomolar Binding Affinities Based upon a New Scaffold. J Med Chem. 2012
18. Roth BD, Blankley CJ, Chucholowski AW, Ferguson E, Hoefle ML, Ortwine DF, Newton RS, Sekerke CS, Sliskovic DR, Stratton CD, et al. Inhibitors of cholesterol biosynthesis. 3.

Tetrahydro-4-hydroxy-6-[2-(1H-pyrrol-1-yl)ethyl]-2H-pyran-2-one inhibitors of HMG-CoA reductase. 2. Effects of introducing substituents at positions three and four of the pyrrole nucleus. J Med Chem. 1991; 34:357–366. [PubMed: 1992137]

19. Zhang H, Cai Q, Ma D. Amino acid promoted CuI-catalyzed C-N bond formation between aryl halides and amines or N-containing heterocycles. J Org Chem. 2005; 70:5164–5173. [PubMed: 15960520]
20. Bruncko M, Oost TK, Belli BA, Ding H, Joseph MK, Kunzer A, Martineau D, McClellan WJ, Mitten M, Ng SC, Nimmer PM, Oltersdorf T, Park CM, Petros AM, Shoemaker AR, Song X, Wang X, Wendt MD, Zhang H, Fesik SW, Rosenberg SH, Elmore SW. Studies leading to potent, dual inhibitors of Bcl-2 and Bcl-xL. J Med Chem. 2007; 50:641–662. [PubMed: 17256834]
21. Hartwig JF, Kawatsura M, Hauck SI, Shaughnessy KH, Alcazar-Roman LM. Room-Temperature Palladium-Catalyzed Amination of Aryl Bromides and Chlorides and Extended Scope of Aromatic C-N Bond Formation with a Commercial Ligand. J Org Chem. 1999; 64:5575–5580. [PubMed: 11674624]
22. Nikolovska-Coleska Z, Wang R, Fang X, Pan H, Tomita Y, Li P, Roller PP, Krajewski K, Saito NG, Stuckey JA, Wang S. Development and optimization of a binding assay for the XIAP BIR3 domain using fluorescence polarization. Anal Biochem. 2004; 332:261–273. [PubMed: 15325294]
23. Huang X. Fluorescence polarization competition assay: the range of resolvable inhibitor potency is limited by the affinity of the fluorescent ligand. J Biomol Screen. 2003; 8:34–38. [PubMed: 12854996]
24. Lee EF, Czabotar PE, Smith BJ, Deshayes K, Zobel K, Colman PM, Fairlie WD. Crystal structure of ABT-737 complexed with Bcl-xL: implications for selectivity of antagonists of the Bcl-2 family. Cell Death Differ. 2007; 14:1711–1713. [PubMed: 17572662]
25. Jones G, Willett P, Glen RC, Leach AR, Taylor R. Development and validation of a genetic algorithm for flexible docking. J Mol Biol. 1997; 267:727–748. [PubMed: 9126849]
26. Verdonk ML, Cole JC, Hartshorn MJ, Murray CW, Taylor RD. Improved protein-ligand docking using GOLD. Proteins. 2003; 52:609–623. [PubMed: 12910460]
27. Sybyl; a molecular modeling system; is supplied by Tripos, I, St. Louis, MO 63144.
28. Otwinowski, Z.; Minor, W. [20] Processing of X-ray diffraction data collected in oscillation mode. In: Carter, Charles W., Jr, editor. Methods in Enzymology. Vol. 276. Academic Press; 1997. p. 307-326.
29. McCoy AJ, Grosse-Kunstleve RW, Adams PD, Winn MD, Storoni LC, Read RJ. Phaser crystallographic software. J Appl Crystallogr. 2007; 40:658–674. [PubMed: 19461840]
30. Bricogne, G.; Blanc, E.; Brandl, M.; Flensburg, C.; Keller, P.; Paciorek, W.; Roversi, P.; Sharff, A.; Smart, O.; Vonrhein, C.; Womack, T. BUSTER, version 2.9. Global Phasing Ltd; Cambridge, United Kingdom: 2010.
31. Emsley P, Cowtan K. Coot: model-building tools for molecular graphics. Acta Crystallogr Sect D Biol Crystallogr. 2004; 60:2126–2132. [PubMed: 15572765]
32. Schuttelkopf AW, van Aalten DM. PRODRG: a tool for high-throughput crystallography of protein-ligand complexes. Acta Crystallogr Sect D Biol Crystallogr. 2004; 60:1355–1363. [PubMed: 15272157]

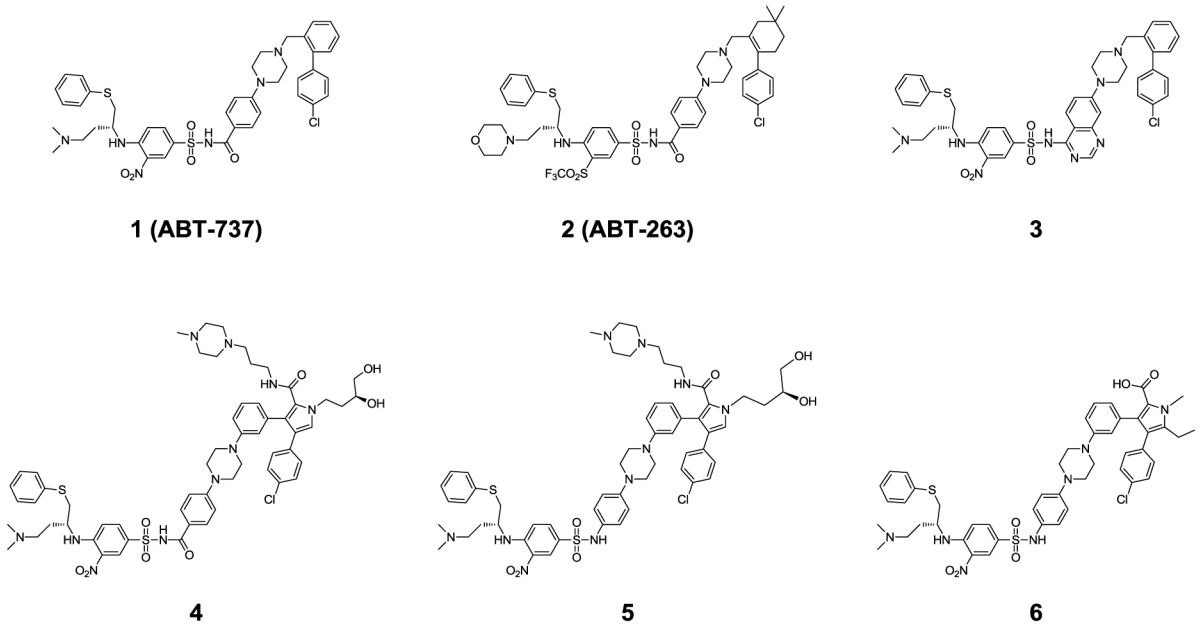


**Figure 1.**
Chemical structures of previously reported Bcl-2/Bcl-xL inhibitors.

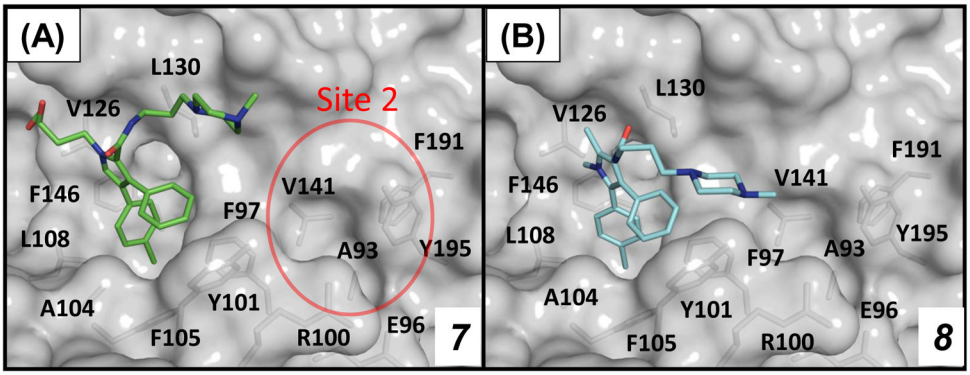


**Figure 2.**

(**A**) Co-crystal structure of **7** in complex with Bcl-xL (1.7 Å). (**B**) Predicted binding model of **8** in complex with Bcl-xL.

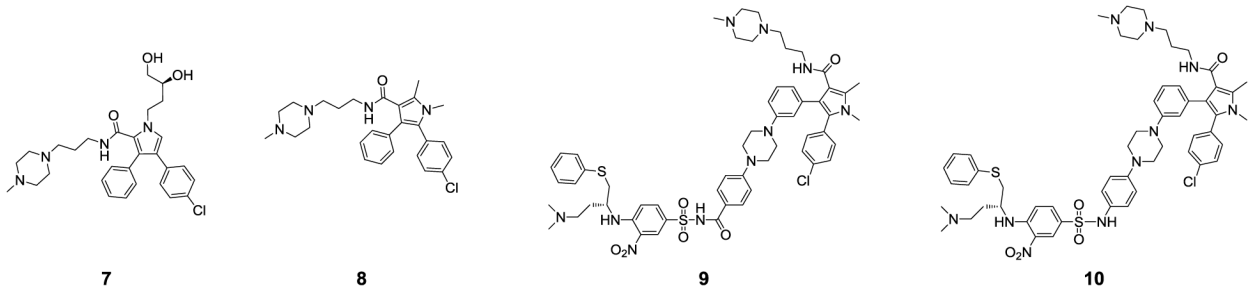


**Figure 3.**
Chemical structures of **7** and newly designed Bcl-2/Bcl-xL inhibitors.

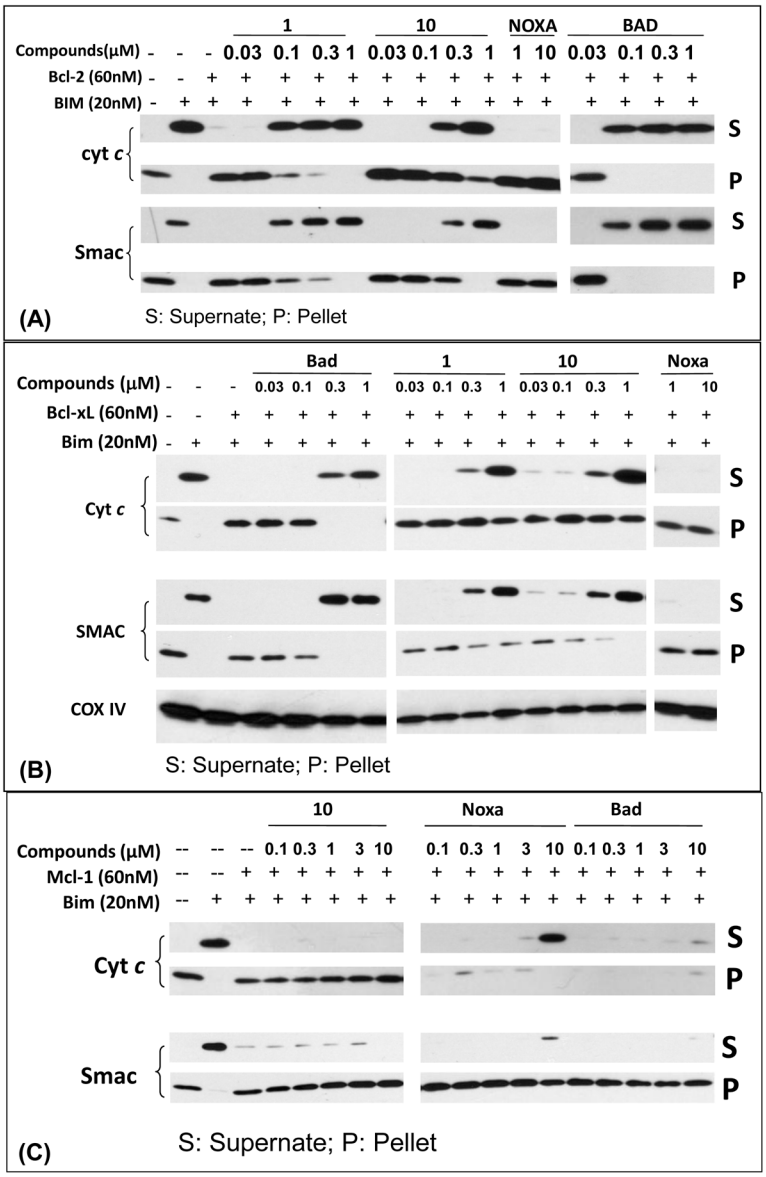


**Figure 4.**

Functional antagonism against Bcl-2 (A), Bcl-xL (B) and Mcl-1 (C) proteins by **10**, **1**, BAD and NOXA BH3 peptides in cell-free system. While **1**, **10**, and BAD can effectively antagonize Bcl-2 and Bcl-xL to restore the release of cytochrome c (Cyt c) and Smac proteins from mitochondria induced by the Bim BH3 peptide, Noxa fails to do so. Conversely, while **10** and BAD fail to antagonize Mcl-1 to restore the release of Cyt c and Smac proteins from mitochondria induced by the Bim BH3 peptide, Noxa can effectively do so. COX IV was used as the loading control in (B).

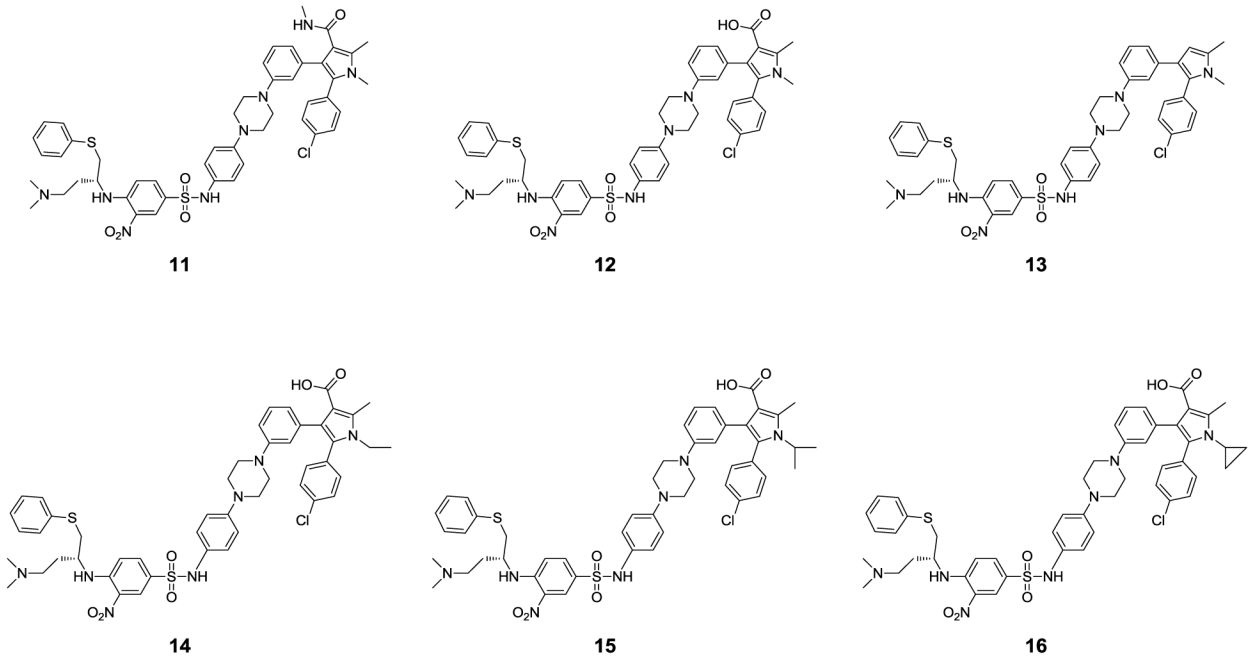


**Figure 5.**
Chemical structures of new analogues of **10**.

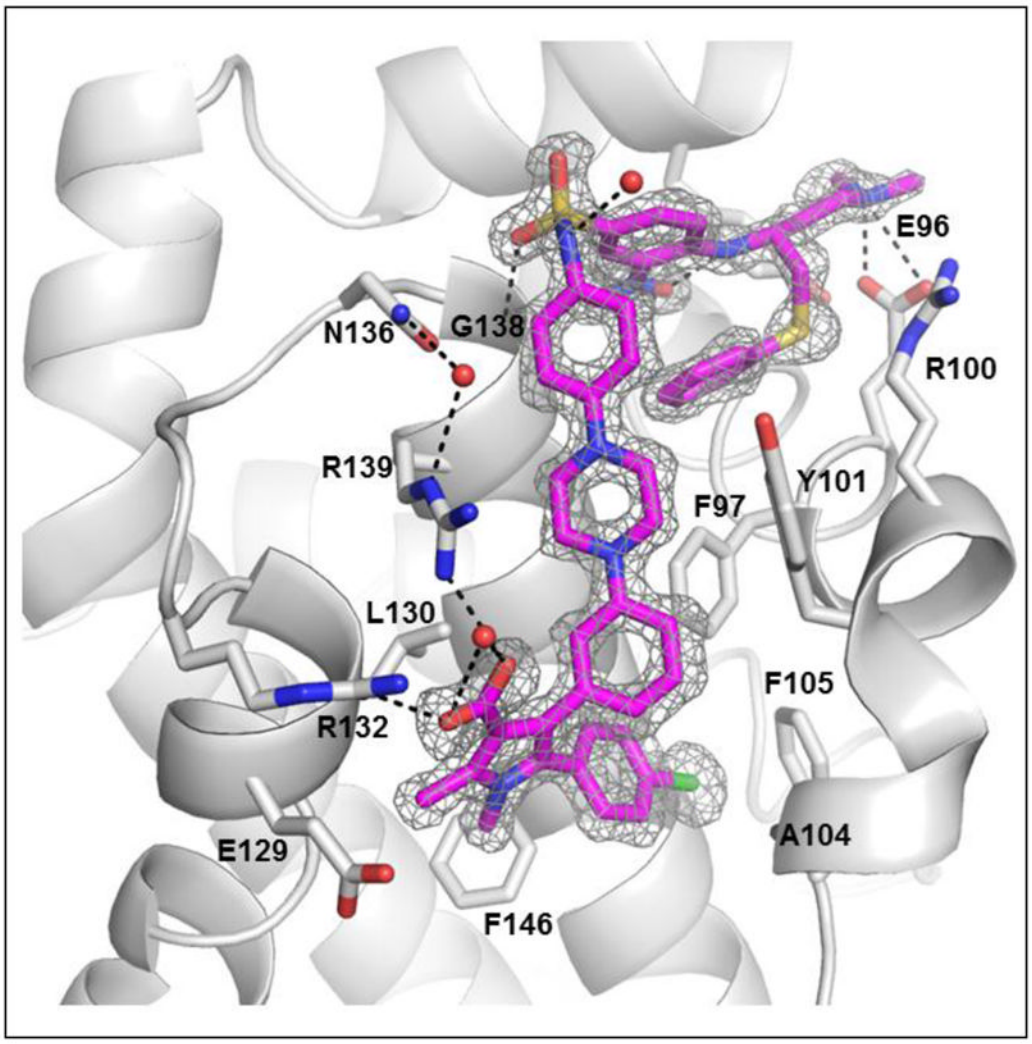


**Figure 6.**
A crystal structure of **12** complexed with Bcl-xL at 1.4 Å resolution. Compound **12** in cyan; key residues interacting in Bcl-xL in grey; oxygens in red; nitrogens in blue, sulphur in yellow and chlorine in green.

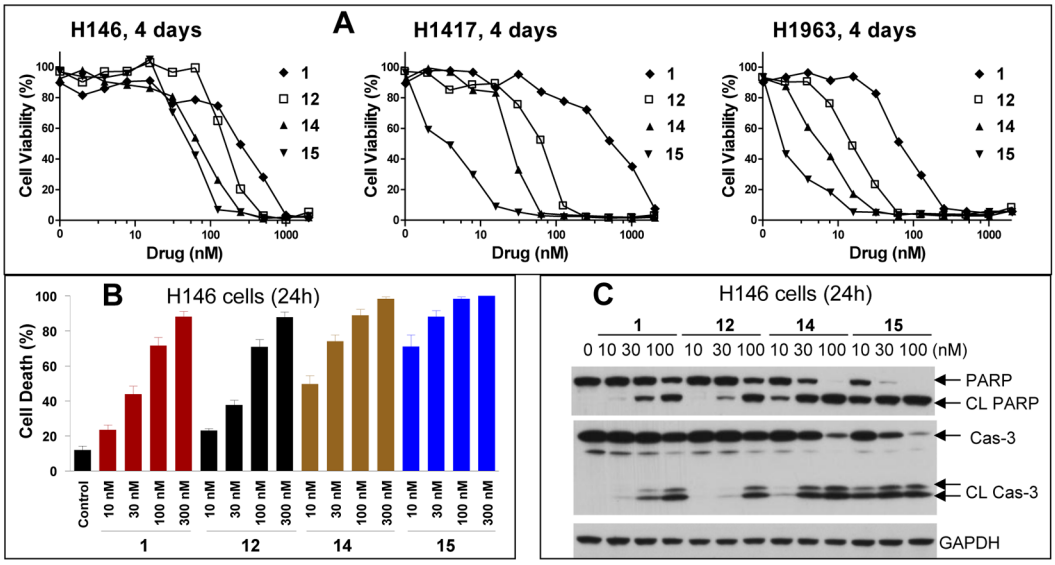


**Figure 7.**

(**A**). Representative cell growth inhibition of **12**, **14**, **15** and **1** in three small-cell lung cancer cell lines. (**B**). Cell death induction by **12**, **14**, **15** and **1** in H146 cell line. Cells were treated for 24 h and cell death was analyzed by trypan blue assay. (**C**). Induction of cleavage of PARP and caspase-3 in H146 cell line by **12**, **14**, **15** and **1**. Cells were treated for 24 h and caspase-3 (Cas 3) and PARP were probed by western blotting. Cl PARP, cleaved PARP; Cl Cas 3 (cleaved caspase-3). GAPDH was used as the loading control.

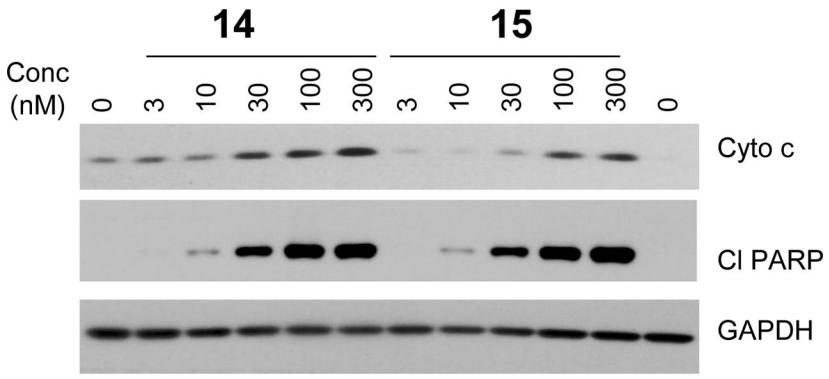


**Figure 8.**

Analysis of cytochrome C (Cyto C) release from mitochondria into cytosol and cleavage of PARP (Cl PARP) induced by **14** and **15** in H146 cells in 2 h. GAPDH was used as the loading control.

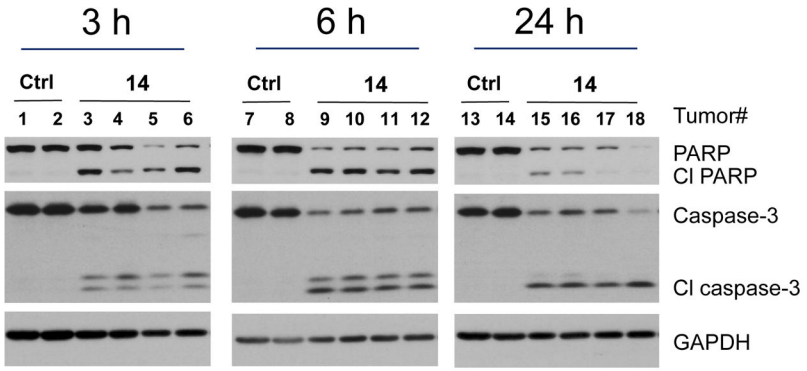


**Figure 9.**

Analysis of induction of cleavage of PARP and caspase-3 in the H146 xenograft tumor tissues by **14** (25 mg/kg, *i.v.*). Mice bearing H146 xenograft tumors were dosed with either **14** or vehicle. Animals were sacrificed at 3, 6 and 24 hr time-points and tumor tissues were analyzed by western blot for cleavage of PARP (Cl PARP) and caspase-3 (Cl caspase-3). GAPDH was used as the loading control.

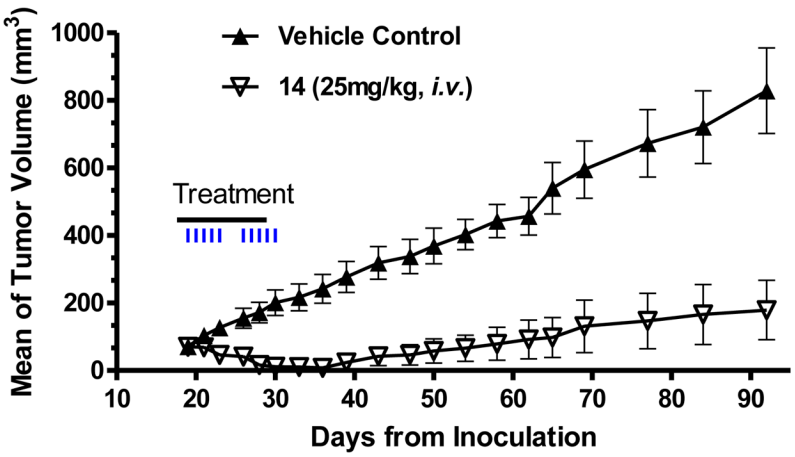


**Figure 10.**

Antitumor activity of compound **14** in H146 xenograft model. H146 tumor cells were injected subcutaneously into SCID mice and treatments started when tumors reached a mean volume of 70 $mm^3$. Each group consisted of 8 mice/tumors.

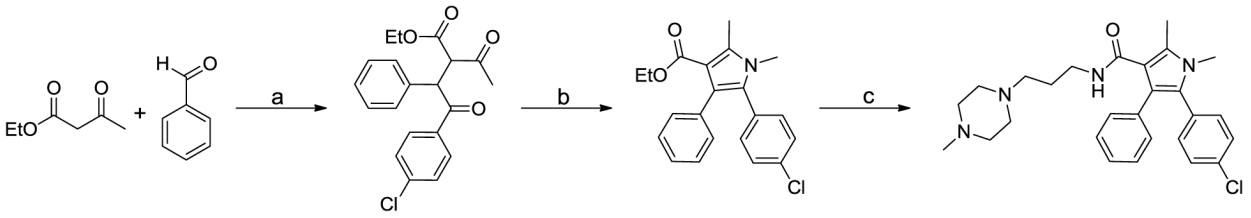


**17** **18** **8**

**Scheme 1.**

Synthesis of compound **8**.

Reagents and conditions: a) i. Piperidine, AcOH, Toluene; ii. 4-chlorobenzaldehyde, 3-ethyl-5-(2-hydroxyethyl)-4-methylthiazol-3-ium bromide, $Et_3N$, 70 °C; b) $MeNH_2$, MeOH, then HCI, rt; c) i. NaOH, Dioxane, EtOH, $H_2O$, reflux; ii. 3-(4-methylpiperazin-1-yl)propan-1-amine, EDCl, HOBt, DIEA, DCM.

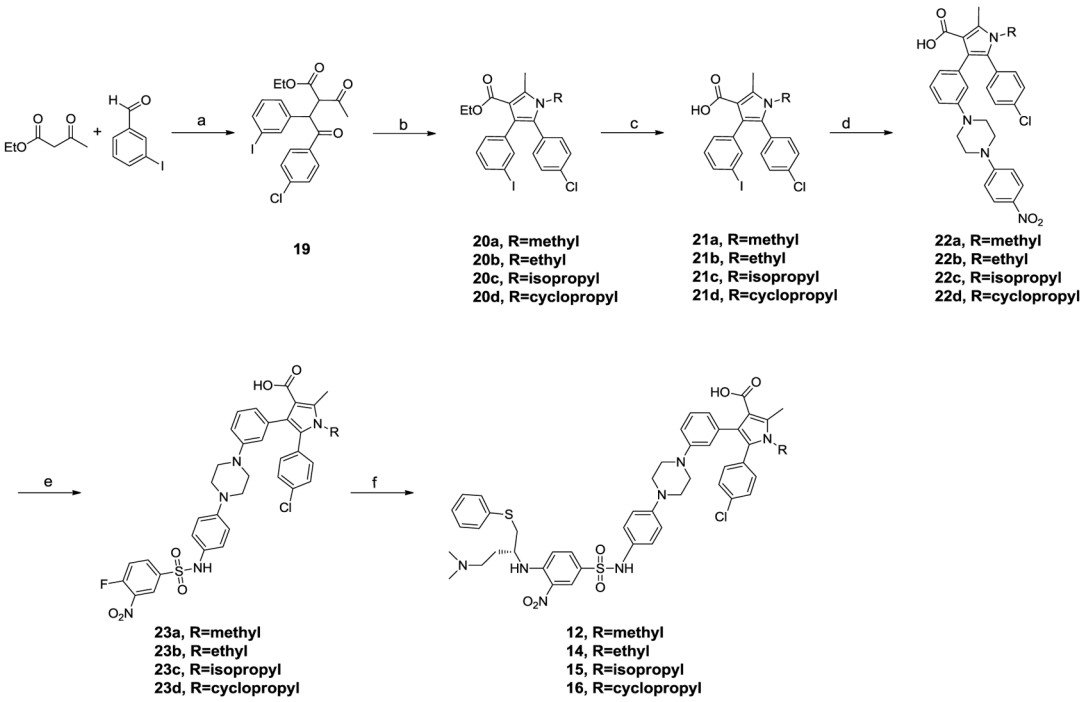


**Scheme 2.**

Synthesis of compounds **12**, **14**, **15** and **16**.

Reagents and conditions: a) i. Piperidine, AcOH, Toluene; ii. 4-chlorobenzaldehyde, 3-ethyl-5-(2-hydroxyethyl)-4-methylthiazol-3-ium bromide, $Et_3N$, 70 °C; b) $RNH_2$, MeOH; c) NaOH, Dioxane, EtOH, $H_2O$, reflux; d) 1-(4-nitrophenyl)piperazine, CuI, L-Proline, $K_2CO_3$, 80 °C, overnight; e) i. $H_2$, Pd/C; ii. 4-fluoro-3-nitrobenzene-1-sulfonyl chloride, pyridine; f) (*R*)-$N^1$,$N^1$-dimethyl-4-(phenylthio)butane-1,3-diamine, DIPEA, DMF

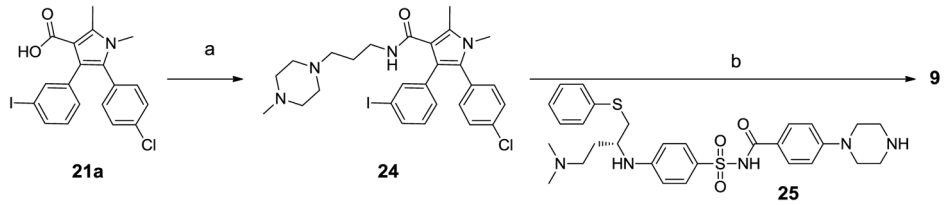


**Scheme 3.**

Synthesis of compound **9**.

Reagents and conditions: a) 3-(4-methylpiperazin-1-yl)propan-1-amine, EDCl, HOBt, DIEA, DCM; b) $Pd(dba)_2$, tri-tert-butylphosphine, sodium tert-butoxide, DMF, toluene;

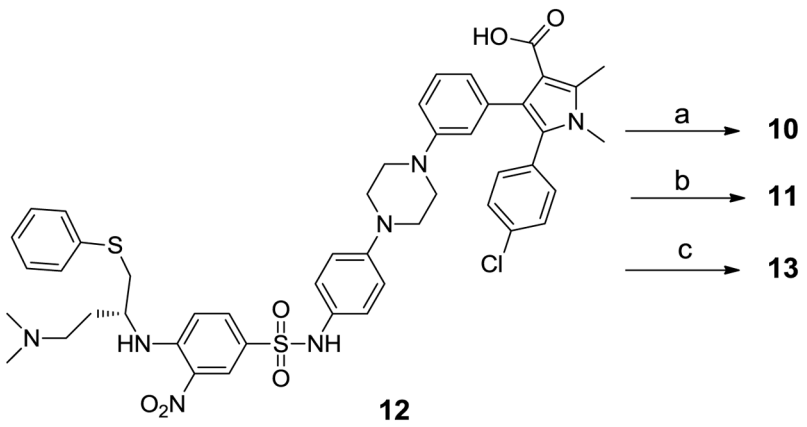


**Scheme 4.**

Synthesis of compounds **10**, **11** and **13**.

Reagents and conditions: a) 3-(4-methylpiperazin-1-yl)propan-1-amine, EDCl, HOBt, DIEA, DCM; b) methyl amine, EDCl, HOBt, DIEA, DCM, c) TFA, $CH_2Cl_2$;

**Table 1**

Binding affinities of designed and reference compounds to Bcl-2, Bcl-xL and Mcl-1 proteins and inhibition of cell growth in three small-cell lung cancer cell lines.

| CPDS | Binding Affinities | | | | | Cell Growth Inhibition ($IC_{50}$ ± SD, nM) | | |
|---|---|---|---|---|---|---|---|---|
| | Bcl-2 | | Bcl-xL | | Mcl-1 | | | |
| | $IC_{50}$ ± SD (nM) | $K_i$ ± SD (nM) | $IC_{50}$ ± SD (nM) | $K_i$ ± SD (nM) | $IC_{50}$ ± SD | H146 | H1417 | H1963 |
| **6** | 4.1 ± 0.7 | 0.82 ± 0.19 | 7.5 ± 1.3 | < 1 | > 2 (μM) | 61 ± 9 | 90 ±3 | n.t. |
| **7** | 213±16 (μM) | 78 ±6 (μM) | 453 ±25 (μM) | 138±8 (μM) | >100 (μM) | >10,000 | >10,000 | >10,000 |
| **8** | 103 ±26 (μM) | 38 ±10 (μM) | 291 (μM) | 88 (μM) | >100 (μM) | >10,000 | >10,000 | >10,000 |
| **9** | 29 ± 8 | 7 ± 2 | 5 ± 2 | < 1 | > 100 (μM) | >10,000 | >10,000 | >10,000 |
| **10** | 2 ± 0.6 | < 0.6 | 9 ± 2 | < 1 | >10 (μM) | 110 ± 42 | 258 ± 43 | 72 ± 6 |
| **1** | 2 ± 0.2 | < 0.6 | 6 ± 2 | < 1 | > 1 (μM) | 37±29 | 412±100 | 59±15 |
| **11** | 5 ± 1 | 1.1 ± 0.2 | 6 ± 3 | < 1 | > 10 (μM) | 36 ± 26 | 109 ± 10 | 30 ± 12 |
| **12** | 1.3 ±0.2 | < 0.6 | 6 ±1 | < 1 | > 2 (μM) | 61±39 | 93±27 | 19±7 |
| **13** | 99 ±5 | 25 ±2 | 11 ±6 | 1.2 ±0.6 | > 10 (μM) | >10,000 | 9229±793 | 6475±5269 |
| **14** | 2 ± 1.6 | < 0.6 | 6.6 ± 2.3 | < 1 | > 2 (μM) | 8.1±3.5 | 17.7±9.5 | 4.5±2.2 |
| **15** | 1.4 ± 0.5 | < 0.6 | 4.8 ± 0.1 | < 1 | > 2 (μM) | 3.0±2.4 | 3.4±1.1 | 1.9± 0.9 |
| **16** | 17.6 ± 2.2 | 4.3 ± 0.6 | 7.7 ± 0.9 | < 1 | > 2 (μM) | 69 ±21 | 154 ±19 | 60±5 |
| BIM | < 1 | < 0.6 | < 1 | < 1 | 5 ± 1 (nM) | n.t. | n.t. | n.t. |
| BAD | 40 ± 8 | 10 ± 2 | 5 ± 0.3 | < 1 | 32 ± 2 (μM) | n.t. | n.t. | n.t. |
| NOXA | 16.7±0.8 (μM) | 3.6 (μM) | 11.0±1.7 (μM) | 3.4 (μM) | 37 ± 3 (nM) | n.t. | n.t. | n.t. |